Plexins Promote Hedgehog Signaling Through Their Cytoplasmic GAP Activity

Justine M. Pinskey[1*], Tyler M. Hoard[1*], Xiao-Feng Zhao[1], Nicole E. Franks[1], Zoë C. Frank[1], Alexandra N. McMellen[1], Roman J. Giger[1,2], and Benjamin L. Allen[1]

[1]Department of Cell and Developmental Biology, [2]Department of Neurology, University of Michigan, Ann Arbor, MI. 48109, USA

* These authors contributed equally.

Correspondence: Benjamin L. Allen, benallen@umich.edu

Running Title: Plexins Promote Hedgehog Signaling

Abstract

Hedgehog signaling controls tissue patterning during embryonic and postnatal development and continues to play important roles throughout life. Characterizing the full complement of Hedgehog pathway components is essential to understanding its wide-ranging functions. Previous work has identified Neuropilins, established Semaphorin receptors, as positive regulators of Hedgehog signaling. Neuropilins require Plexin co-receptors to mediate Semaphorin signaling, but a role for Plexins in Hedgehog signaling has not yet been explored. Here, we provide evidence that multiple Plexins promote Hedgehog signaling in NIH/3T3 fibroblasts and that Plexin loss-of-function in these cells results in significantly reduced Hedgehog pathway activity. Catalytic activity of the Plexin GTPase activating protein (GAP) domain is required for Hedgehog signal promotion, and constitutive activation of the GAP domain further amplifies Hedgehog signaling. Additionally, we demonstrate that Plexins promote Hedgehog signaling at the level of GLI transcription factors and that this promotion requires intact primary cilia. Finally, we find that Plexin loss-of-function significantly reduces the response to Hedgehogα pathway activation in the mouse dentate gyrus. Together, these data identify Plexins as novel components of the Hedgehog pathway and provide insight into their mechanism of action.

Introduction

The Hedgehog (HH) signaling pathway utilizes a core set of components to coordinate diverse cellular processes. In the absence of HH ligand, the twelve-pass transmembrane protein Patched 1 (PTCH1) inhibits pathway activity by repressing a second cell-surface protein Smoothened (SMO), a seven-pass transmembrane protein with GPCR-like activity (Alcedo et al. 1996; Marigo and Tabin 1996; Stone et al. 1996; van den Heuvel and Ingham 1996). HH ligand binding to PTCH1 leads to de-repression of SMO, which shifts the processing of GLI transcription factors from repressor to activator forms, thus altering the balance of HH target gene expression (Hui and Angers 2011). By balancing the activity of these key molecules, HH signaling directs embryonic and postnatal development as well as adult tissue homeostasis in a wide variety of cellular contexts. In contrast, HH pathway disruption can drive a number of diseases, including cancer (Teglund and Toftgard 2010; Briscoe and Therond 2013; Petrova and Joyner 2014).

Beyond these core pathway components, a growing list of additional proteins regulate HH signaling at the cell surface in a tissue- and stage-specific manner (Beachy et al. 2010). Some examples include growth arrest-specific 1 (GAS1); CAM-related/downregulated by oncogenes (CDON); brother of CDON (BOC); PTCH1 homolog Patched 2 (PTCH2); Hedgehog interacting protein (HHIP); Dispatched (DISP); Signal peptide, CUB domain, EGF-like 2 (Scube2); G-protein-coupled-receptor 161 (GPR161); glypicans (GPCs); and low-density lipoprotein receptor-related 2 (LRP2) (Burke et al. 1999; Caspary et al. 2002; Kawakami et al. 2002; Ma et al. 2002; Jeong and McMahon 2005; Kawakami et al. 2005; Woods and Talbot 2005; Hollway et al. 2006;

Vyas et al. 2008; Yan and Lin 2008; Christ et al. 2012; Creanga et al. 2012; Tukachinsky et al. 2012; Mukhopadhyay et al. 2013; Bandari et al. 2015; Christ et al. 2015). Notably, many of these components act redundantly to mediate HH signal transduction (Zhang et al. 2001; Jeong and McMahon 2005; Allen et al. 2007; Allen et al. 2011; Izzi et al. 2011; Holtz et al. 2013). As a result, previous genetic screens may have missed additional regulators of the HH pathway due to their redundant nature. Furthermore, gene duplication events and increased complexity within vertebrate HH signaling, including a requirement for the primary cilium, have made it difficult to study HH regulators that lack invertebrate counterparts, such as Scube2 and GAS1. Therefore, our overall understanding of HH regulation remains incomplete.

The Semaphorins (SEMA) are a large family of membrane-bound and secreted proteins that regulate cell migration, axon guidance, synapse assembly, angiogenesis, immune function, and cell death (Yazdani and Terman 2006; Jongbloets and Pasterkamp 2014; Koropouli and Kolodkin 2014; Fard and Tamagnone 2021). NRPs directly interact with class 3 SEMA ligands and require Plexin (PLXN) co-receptors to transduce SEMA signals intracellularly (Chen et al. 1997; He and Tessier-Lavigne 1997; Kolodkin et al. 1997; Takahashi et al. 1999; Tamagnone et al. 1999; Gu et al. 2005). Membrane-bound SEMA and Sema3E interact directly with PLXN extracellular domains to activate downstream signaling events, which lead to remodeling and disassembly of the cytoskeleton (Barberis et al. 2004; Neufeld and Kessler 2008; Jongbloets and Pasterkamp 2014; Rich et al. 2021). PLXNs are a family of conserved, single-pass transmembrane proteins containing nine different receptor types, which fall into four subfamilies based on homology (A, B, C, and D) (Tamagnone et al. 1999). The cytoplasmic domain of all

PLXN family members harbors a GTPase activating protein (GAP) domain (Rohm et al. 2000b; Wang et al. 2012). Catalytic activity of the PLXN GAP domain is necessary for SEMA mediated cytoskeletal remodeling and cell migration (Hota and Buck 2012; Wang et al. 2013; Zhao et al. 2018). Importantly, there is a mechanistic link between HH and NRPs. Multiple lines of evidence show that NRPs positively regulate HH signaling through their cytoplasmic domains (Ge et al., 2015; Hillman et al., 2011; Pinskey et al., 2017); however, a role for PLXNs in HH signaling remains unexplored.

Here, we investigated a role for PLXNs in HH pathway regulation. Our data suggest that multiple PLXNs, including members of the PLXN A and B subfamilies, positively regulate HH signaling. Similar to NRPs, we find that the PLXN cytoplasmic domain is necessary for HH regulation. Interestingly, while the mechanism of NRP action in HH signaling may diverge from its mechanism in SEMA signaling (Andreyeva et al. 2011; Ge et al. 2015; Pinskey et al. 2017), we discover that PLXNs function similarly in SEMA and HH cascades. Mutating key residues within the cytoplasmic PLXN GAP domain prevents PLXN from promoting HH signaling. Further, deleting the PLXN extracellular domain to create a constitutively active receptor augments HH promotion and alters HH-dependent tissue patterning and cell migration in the embryonic chicken neural tube, suggesting that PLXNs positively regulate HH signaling through GAP enzymatic activity. Additionally, we determine that PLXNs act at the level of the GLI transcription factors, and that PLXNs require intact primary cilia to promote HH pathway activity. In the developing mouse hippocampus, we observe PLXN dependent regulation of HH target gene expression in the dentate gyrus, *in vivo*. Taken together, these data

identify PLXNs as novel components of the HH pathway and contribute to our mechanistic understanding of HH regulation at the cell surface.

Results

Multiple Plxns promote HH signaling in NIH/3T3 fibroblasts

PLXNs consist of nine members that can be classified into four different subfamilies based on homology (PLXNA1-4, PLXNB1-3, PLXNC1, and PLXND1) (Tamagnone et al. 1999; Neufeld and Kessler 2008). PLXNs from the A and D subfamilies interact with NRP co-receptors (Takahashi et al. 1999; Neufeld and Kessler 2008), which have been previously identified as positive regulators of HH signaling (Hillman et al. 2011; Ge et al. 2015; Pinskey et al. 2017). We initially investigated whether *Plxna1* expression in HH-responsive NIH/3T3 fibroblasts would impact HH signaling using a luciferase reporter assay ((Nybakken et al. 2005); Figure 1A). Strikingly, and similar to what we previously observed with *Nrp1* (Pinskey et al. 2017), *Plxna1* expression significantly increases HH pathway activation compared to a vector-transfected control (Figure 1B). Of note, PLXNA1 does not promote HH signaling in the absence of pathway activation with HH ligand (Figure 1B). To address whether HH promotion was specific to PLXNA1, we also examined PLXNA2, PLXNA3, and PLXNA4. Our data suggest that all members of the PLXN A subfamily promote HH signaling following pathway activation with HH ligand (Figure 1C-E). We extended our analyses to include PLXNB2, which is not known to interact with NRPs (Neufeld and Kessler 2008). Surprisingly, PLXNB2 also promotes HH signaling to a similar extent as PLXNs from the A subfamily, suggesting that PLXN-mediated HH promotion may be

124 independent of NRP interaction (Figure 1F-G). Importantly, GFRα1, an unrelated cell-
125 surface protein within the glial cell line-derived neurotrophic factor receptor (GFR)
126 family, does not promote HH signaling (Figure 1G). Taken together, these data suggest
127 that multiple PLXN family members promote HH signaling in NIH/3T3 cells.
128
129 *Plxn knockdown decreases HH-responsiveness in NIH/3T3 fibroblasts*
130 According to RNA sequencing data from the ENCODE project (Consortium
131 2012; Davis et al. 2018), NIH/3T3 fibroblasts express a subset of Plxns at varying levels,
132 with *Plxna1* and *Plxnb2* most highly expressed, followed by *Plxnd1*, *Plxna3*, and *Plxna2*
133 (Figure S1). To address the effect of endogenous PLXNs on HH signaling in NIH/3T3
134 cells, we generated two different *Plxna1*$^{-/-}$;*Plxna2*$^{-/-}$ mouse embryonic fibroblast lines
135 from embryonic day (E) 14.5 mouse embryos (Todaro and Green 1963). We then used
136 quantitative, real-time polymerase chain reaction (RT-qPCR) to analyze HH target gene
137 expression in fibroblasts treated with a SMO agonist (SAG; Figure 1H-I). In each
138 experiment, we used BLOCK-iT™ fluorescent oligos to visually confirm transfection,
139 and we compared each result to an internal BLOCK-iT™ transfected control (Figure 1H-
140 I). Therefore, fold changes in expression are relative within each experiment and should
141 not be compared across panels. Interestingly, both cell lines lacking *Plxna1* and *Plxna2*
142 still respond to SAG activation of HH signaling, as measured by expression of the direct
143 HH transcriptional targets, *Gli1* and *Ptch1* (Figure 1H-I). We hypothesized that this was
144 likely due to the presence of other Plxn family members, which could compensate for the
145 lack of PLXNA1 and PLXNA2.

To address the potential functional redundancy of other Plxn family members, we used siRNA reagents to reduce levels of *PlxnB2*, *PlxnA3*, and *PlxnD1* in *Plxna1*$^{-/-}$;*Plxna2*$^{-/-}$ cells. Strikingly, both cell lines treated with the *Plxn* siRNAs listed above showed significantly reduced responses to SAG activation of *Gli1* and *Ptch1* compared to BLOCK-iT™ controls (Figure 1H-I). The degree of reduction following *Plxn* depletion is similar to that observed with *Nrp* depletion using previously published siRNA reagents targeting *Nrp1* and *Nrp2* (Hillman et al. 2011) (Figure 1H-I). Together, these data suggest that, like NRPs, PLXNs are required for HH signal transduction in NIH/3T3 fibroblasts.

The PLXNA1 transmembrane and cytoplasmic domains are necessary for HH signal promotion

PLXNs are single-pass transmembrane proteins containing an extracellular domain (ECD) that can interact with NRPs and SEMA ligands, a transmembrane (TM) domain that mediates dimerization, and a cytoplasmic domain (CD) through which PLXNs signal intracellularly (Neufeld and Kessler 2008). While many HH regulators at the cell surface bind to HH ligands through their ECD (Lee et al. 2001; Tenzen et al. 2006; Capurro et al. 2008; Chang et al. 2011; Izzi et al. 2011; Christ et al. 2012; Whalen et al. 2013), NRP1 acts through its CD to regulate HH signaling (Ge et al. 2015; Pinskey et al. 2017). To investigate the mechanism of PLXN action in HH signaling, we first asked whether the PLXN CD is required for HH promotion. Interestingly, deleting the PLXNA1 TM and CD (PLXNA1$^{\Delta TMCD}$) or the CD alone (PLXNA1$^{\Delta CD}$) abrogates PXLNA1-mediated promotion of HH signaling in NIH/3T3 cells (Figure 2A-B). Western blot analyses confirmed PLXNA1, PLXNA1$^{\Delta TMCD}$, and PLXNA1$^{\Delta CD}$ expression and

169 PLXNA1$^{\Delta TMCD}$ secretion (Figure 2C). Further, immunofluorescence staining for an
170 extracellular MYC epitope under permeabilizing and non-permeabilizing conditions
171 confirmed the cell surface localization of PLXNA1 and PLXNA1$^{\Delta CD}$ as well as the
172 secretion of PLXNA1$^{\Delta TMCD}$, as compared to a control BOC construct with a C-terminal
173 MYC tag (Figure 2D-K). These results suggest that the PLXNA1 TM and CD are
174 required for promotion of HH signaling.
175
176 *PLXN cytoplasmic GAP activity mediates HH signal promotion*
177 Upon binding to the PLXN extracellular SEMA domain, SEMA ligand triggers a
178 conformational change, releasing PLXN autoinhibition and allowing for the full
179 activation of the intracellular GAP (Takahashi and Strittmatter 2001; Janssen et al. 2010;
180 Nogi et al. 2010). As a result, deleting the autoinhibitory PLXN ECD results in
181 constitutively GAP activity that induces robust cytoskeletal collapse through downstream
182 signaling events (Takahashi and Strittmatter 2001; Hota and Buck 2012). To further test
183 whether PLXN GAP function regulates HH signaling, we deleted the PLXNA1 ECD
184 (PLXNA1$^{\Delta ECD}$) and measured HH-dependent luciferase reporter activity in NIH/3T3 cells
185 (Figure 3A). Not only is PLXNA1$^{\Delta ECD}$ still able to promote HH signaling, but the
186 constitutively active PLXN GAP domain significantly augments the level of HH
187 promotion (Figure 3B). While full-length PLXN boosts HH signaling one and a half to
188 two-fold on average, PLXNA1$^{\Delta ECD}$ consistently increases the level of HH signaling
189 between four- and ten-fold, averaging an approximately six-fold increase (Figure S2A).
190 The PLXN CD is essential for intracellular SEMA signal transduction, acting
191 through a split GAP domain to induce cytoskeletal collapse (Puschel 2007; Neufeld and

Kessler 2008; Duan et al. 2014). Arginine to alanine mutations in residues 1429 and 1430 of mouse PLXNA1 disrupt GAP activity, rendering PLXNA1 a nonfunctional SEMA receptor in a COS7 cell collapse assay (Rohm et al. 2000a). Strikingly, recapitulating these conserved arginine mutations within the PLXNA1 GAP domain also rendered PLXNA1 unable to promote HH signaling (PLXNA1R1; Figure 3C). Importantly, analogous mutations in PLXNB2 also abrogate the promotion of HH pathway activity (PLXNB2R1; Figure S2B-C). Further, the A1R1 arginine to alanine GAP mutations in the context of the PLXNA1 ECD deletion significantly reduces the level of HH promotion, though it does not completely abrogate PLXN-mediated HH pathway induction when compared with PLXNA1$^{\Delta CD}$ (Figure 3D). Immunofluorescence analyses indicated appropriate localization of these constructs to the cell surface, compared to a C-terminally tagged BOC control, as well as cytoskeletal collapse in PLXNA1$^{\Delta ECD}$ and to some extent PLXNA1, with the expected lack of collapse in PLXNA1R1$^{\Delta ECD}$ and PLXNA1$^{\Delta CD}$ (Figure 3E-N; Figure S2D-G). Together, these results suggest that GAP activity is necessary for PLXN-mediated promotion of HH signaling.

PLXNA1 promotes HH signaling at the level of GLI activation

HH signaling culminates in the differential processing and activation of the GLI family of transcription factors, which shuttle in and out of the primary cilium and are phosphorylated by several kinases to regulate their activity (Hui and Angers 2011). Transfecting *SmoM2*, a constitutively active form of Smoothened, or *Gli1*, an obligate HH activator, into our luciferase reporter assay in NIH/3T3 cells results in tens to thousands of fold induction of HH reporter activity, respectively. Still, co-transfecting

215 *SmoM2* or *Gli1* with *Plxna1*$^{\Delta ECD}$ results in a significantly greater HH response (Figure
216 3O-P). Notably, this promotion requires GAP activity as co-transfection of *SmoM2* or
217 *Gli1* with a GAP-deficient *Plxn* (*Plxna1r1*$^{\Delta ECD}$) returns HH pathway activation to near-
218 baseline levels (Figure 3O-P). These data suggest that PLXNs function downstream of
219 HH ligand at the level of GLI regulation, and that full PLXN GAP activation via the
220 release of extracellular autoinhibition is necessary for HH promotion with either *SmoM2*
221 or *Gli1*.
222
223 *PLXNs are not enriched in the primary cilium, but do require primary cilia for HH*
224 *pathway promotion*
225 The primary cilium is an important platform for HH signaling molecules (Wong
226 et al. 2009; Goetz and Anderson 2010) and many HH pathway components, including
227 NRP, are enriched there (Corbit et al. 2005; Haycraft et al. 2005; Rohatgi et al. 2007;
228 Pinskey et al. 2017). Notably, molecules over 40 kDa are unable to freely diffuse into the
229 primary cilium, requiring active transport to enter this highly regulated subcellular
230 compartment (Kee et al. 2012). To test whether PLXNs localize to the primary cilium, we
231 expressed MYC-tagged PLXNs in NIH/3T3 cells and performed immunofluorescent
232 staining for MYC and Acetylated Tubulin (AcTub), which marks the primary cilium.
233 PLXNs are broadly localized throughout the cell (Figure 4A-N), including the cell
234 surface (cf. Figure 3E-N), but are largely excluded from the nucleus. Unlike NRP1,
235 PLXN staining was not enriched within the primary cilium for any of the constructs we
236 tested (Figure 4A-G). Mouse embryonic fibroblasts (MEFs) with a mutation in the dynein
237 heavy chain (*Dync2h1*$^{lln/lln}$) exhibit impaired retrograde transport within the cilium,

allowing for more robust detection of accumulated proteins (Ocbina et al. 2011). However, even in *Dync2h1*$^{lln/lln}$ MEFs, PLXNs still do not accumulate in the primary cilium (Figure 4H-N). These data suggest that PLXN localization to primary cilia is not required to regulate HH signal transduction.

To examine a potential requirement for primary cilia in PLXN-dependent promotion of HH signaling, we performed luciferase assays in WT NIH/3T3 cells as well as *Kif3a*$^{-/-}$ NIH/3T3 cells, which fail to assemble primary cilia (Engelke et al. 2019). As expected, WT NIH/3T3 cells activate HH signaling in response to *SmoM2* transfection, while *Kif3a*$^{-/-}$ NIH/3T3 cells do not (Figure 4O). Notably, *Kif3a*$^{-/-}$ NIH/3T3 cells also do not respond to co-transfection with *SmoM2* and *Plxna1*$^{\Delta ECD}$ (Figure 4O). Both GLI1 and GLI2ΔN have been reported to promote HH pathway activation in the absence of primary cilia (Haycraft et al. 2005; Wong et al. 2009). We confirmed these data by transfecting *Kif3a*$^{-/-}$ NIH/3T3 cells with either *Gli1* or *Gli2ΔN* (Figure 4P). Strikingly, and distinct from what we observe in WT NIH/3T3 cells, co-transfecting *Kif3a*$^{-/-}$ NIH/3T3 cells with either *Gli1* or *Gli2ΔN* and *Plxna1*$^{\Delta ECD}$ displayed no further promotion of HH-signaling (Figure 4P; cf. Figure 3P). These data suggest that, while PLXNs do not localize to the primary cilium, primary cilia are required for PLXN-dependent promotion of HH signaling.

Constitutive Plxn GAP activity drives ectopic cell migration in the embryonic chicken neural tube

The developing spinal cord requires HH signaling for proper patterning and development (Dessaud et al. 2008). SHH, which is initially secreted from the notochord,

signals in a ventral-dorsal gradient to specify distinct cell fates in the neural tube. Notably, SHH also controls cell proliferation and cell migration in this tissue (Cayuso and Marti 2005; Cayuso et al. 2006). Previous work demonstrated that multiple *Plxns* are expressed in the developing chicken neural tube concomitant with SHH-dependent tissue patterning (Mauti et al. 2006). To investigate potential contributions of PLXNs to these SHH-dependent outcomes, we employed chicken *in ovo* neural tube electroporation. While electroporation with an empty vector (*pCIG*) does not impact neural tube patterning (Fig 5A-D), *SmoM2* electroporation drives ectopic expression of NKX6.1 in the dorsal neural tube, a direct target of HH signaling that is normally restricted ventrally (Fig 5E-H). Similarly, electroporation with *Gli1*, an obligate activator of the HH pathway that drives high levels of HH signaling, also results in expansion of the NKX6.1 domain (Figure 5I-L). However, *Gli1* expression also results in ectopic migration of cells into the dorsal lumen of the neural tube, which is typically completely devoid of cells (Figure 5I; yellow asterisk). Electroporation of *Plxna1*$^{\Delta ECD}$ phenocopies *Gli1*-induced migration into the lumen of the neural tube (Figure 5M; yellow asterisk). In some *Plxna1*$^{\Delta ECD}$-electroporated embryos, we observed a minor shift in the NKX6.1 domain (Figure 5P; yellow arrowhead). We also observed a similar trend in the PAX7 domain, which is largely devoid of HH signaling (Figure S3A-I). However, quantitation of the NKX6.1 domain size revealed no significant differences between *pCIG*- and *Plxna1*$^{\Delta ECD}$-electroporated embryos (Figure S3J-M). Further, cells electroporated with *Plxna1*$^{\Delta ECD}$ at the periphery of the endogenous NKX6.1 domain do not express NKX6.1, while cells in this same region that were electroporated with *Gli1* are NKX6.1 positive (Figure S3J-L). Importantly, PLXN-dependent ectopic cell migration is lost upon mutation of the

intracellular PLXN GAP domain (Figure 5Q-T). These data are consistent with our cell signaling assays, which indicate that PLXNs can promote GLI-dependent cellular responses.

Plxna1 or Plxna2 deletion results in decreased numbers of HH-responding cells within the dentate gyrus

Plxns are expressed widely throughout the developing mouse embryo, particularly in the central nervous system (Perala et al. 2005). Interestingly, developing neurons and progenitor cells in the hippocampus express *Plxns* (Cheng et al. 2001) and neuronal progenitor cells rely on HH signaling for proliferation and maintenance, particularly within the dentate gyrus (Machold et al. 2003; Ahn and Joyner 2005). To determine whether PLXNs impact HH signaling in the hippocampus, we crossed *Plxna1* and *Plxna2* deficient mice with a HH-responsive *Gli1lacZ* reporter allele and examined β-galactosidase activity along the rostro-ventral axis of dentate gyrus at postnatal day 7 (P7). Strikingly, *Plxna1*$^{-/-}$ mice have significantly fewer *Gli1*-positive cells in both the dorsal and ventral dentate gyrus compared to their heterozygous littermates (Figure 6A-F). In addition, *Gli1*-positive cells in *Plxna1*$^{-/-}$ mice fail to properly migrate, similar to previously published HH loss-of-function models (Figure 6A-B) (Machold et al. 2003). *Plxna2* deletion has a similar effect on both *lacZ* expression and migration of *Gli1*-positive cells. Significantly fewer β-galactosidase positive cells are detected in the hilus and subventricular zone of the dorsal and ventral dentate gyrus (Figure 6G-L). Together, these data show that PLXNs can regulate HH pathway activation *in vivo* and suggest that multiple PLXNs regulate HH signaling in the developing mouse hippocampus.

Discussion

HH signaling plays important roles in tissue formation, homeostasis and repair, coordinating a number of cellular processes including proliferation, fate specification, and survival (Briscoe and Therond 2013). Canonical SEMA receptors, the NRPs and PLXNs, are expressed in a wide variety of tissues during active HH regulation (Kawasaki et al. 1999; Perala et al. 2005; Mauti et al. 2006; Perala et al. 2012). Here, we present evidence that PLXNs positively regulate HH signaling. Unlike many previously described cell surface HH regulators, which interact directly with HH ligands, PLXNs promote HH signaling through their cytoplasmic domains at the level of GLI regulation (Figure 7). More specifically, we find that GAP enzymatic activity within the PLXN cytoplasmic domain is required for HH promotion, and that constitutive GAP activity further amplifies the HH response. This shows that the PLXN GAP domain is important for canonical SEMA signaling as well as amplification of HH signaling. Further, we find that, while PLXNs themselves do not localize to primary cilia, they require primary cilia to promote HH pathway activity. Finally, our data indicate that increased *Plxn* activity *in ovo* increases cell migration into the neural tube lumen, and *Plxn* deletion *in vivo* results in reduced HH pathway activity in mice. Taken together, we provide multiple lines of evidence for a novel role of PLXNs in HH pathway regulation.

Semaphorin Receptors Act Promiscuously in Multiple Signaling Pathways

While NRPs and PLXNs were first described as SEMA receptors, they also function within other signaling pathways (He and Tessier-Lavigne 1997; Kolodkin et al.

1997; Takahashi et al. 1999; Tamagnone et al. 1999). NRPs play roles in VEGF signaling to regulate angiogenesis, and they interact with a wide variety of proteins, including PIGF-2, heparan sulfate, TGF-β1, HGF, PDGF, FGF, L1-CAM, integrins, and SARS-CoV-2 spike protein (Roth et al. 2008; Prud'homme and Glinka 2012; Muhl et al. 2017; Sarabipour and Mac Gabhann 2021). PLXNs also form complexes with off-track, MET, Ron, scatter factor, and VEGFR2 in various cellular contexts (Winberg et al. 2001; Giordano et al. 2002; Conrotto et al. 2004; Toyofuku et al. 2004). This raises many questions about the nature of these receptors' activities within individual and overlapping signaling contexts. For example, what factors determine whether PLXNs and NRPs function as SEMA receptors and whether the regulate HH signaling? Can these processes happen simultaneously, and if so, how do they influence one another? → Multiple lines of evidence link altered SEMA/PLXN signaling to cancer. Depending on context, aberrant SEMA signaling may promote or suppress tumor growth and lead to various types of cancer (Neufeld et al. 2016). The mechanisms by which altered PLXN signaling influence tumor growth are incompletely understood. A link to increased HH signaling is intriguing because of the well-established role of elevated HH signaling in malignancies.

Another outstanding question is how SEMA ligand impacts HH signaling. A role for SEMA ligands in HH pathway promotion remains unclear as conflicting pieces of evidence exist in the literature. In one study, addition of SEMA ligands in combination with HH ligand or SAG increased HH signaling in NIH/3T3 cells (Ge et al. 2015). Conversely, blocking NRP interaction with SEMA ligand reduces GLI expression (Ge et al. 2015). This model suggests that SEMA ligand increases recruitment of PDE4D to the cell membrane, which interacts with the NRP CD and inhibits PKA, a negative regulator

of GLI proteins (Ge et al. 2015). However, other studies suggest that addition of SEMA ligand has no effect on HH signaling (Hillman et al. 2011), and that NRPs still promote HH signaling when co-transfected with a version of GLI2 that cannot be phosphorylated by PKA at seven important sites (Pinskey et al. 2017). It is important to consider that NIH/3T3 cells, in which these studies were performed, express endogenous PLXNs (Figure S1). Given the results presented here, an alternate explanation of SEMA-mediated HH promotion is that SEMA ligands act through endogenous PLXNs to increase HH reporter activity by stimulating GAP activity. Another discrepancy in the literature concerns the requirement for the NRP ECD in HH promotion (Ge et al. 2015; Pinskey et al. 2017). Again, given that PLXNs promote HH signaling and that the NRP ECD mediates interactions with PLXN co-receptors, the variable effects that have been reported could be explained by the presence of endogenous PLXNs, the level of NRP overexpression, and the sensitivity of the assay.

NRP and PLXN Cooperation in HH Signaling

We previously reported that NRPs promote HH signaling through a novel cytoplasmic motif (Pinskey et al. 2017), within a region of the protein that is dispensable for SEMA signaling (Fantin et al. 2011). This suggests that NRPs may act very differently within SEMA and HH signaling contexts. PLXNs on the other hand, seem to function similarly in HH and SEMA signaling, through cytoplasmic GAP activity. Together, these data raise the question: do NRPs and PLXNs function together or separately in HH signaling? The answer may be both. Several pieces of evidence suggest that NRPs function independently of PLXNs in HH signaling. First, deleting the NRP

ECD, which mediates interaction between NRPs, PLXNs, and SEMA, does not disrupt HH pathway promotion (Pinskey et al. 2017). Furthermore, we report here that PLXNB2 can promote HH signaling, despite its lack of reported interactions with NRPs (Neufeld and Kessler 2008). However, we cannot exclude the possibility that PLXN A subfamily members bind to endogenous NRPs to mediate HH promotion in our assays. Therefore, the ideas that NRPs and PLXNs function independently and together in HH signaling are not mutually exclusive, and additional studies will be required to elucidate their independent and/or cooperative roles.

Connecting PLXN GAP Activity to the HH Pathway

We find that HH pathway activity is regulated by enzymatic activity of the PLXN GAP domain. However, it remains unclear how GAP downstream signaling intersects with the HH signal cascade. The PLXN cytoplasmic domain interacts with a plethora of intracellular proteins, including collapse-response-mediator protein (CRMP) family phosphoproteins, protein kinases, MICAL redox proteins, and small intracellular GTPases from the Rho, Ras, and Rap superfamilies (Puschel 2007; Yang and Terman 2013; Jongbloets and Pasterkamp 2014). Further, our understanding of the cellular mechanisms downstream of the PLXN GAP domain remains incomplete, including which GTPases are regulated by various PLXN family members. This makes it difficult to identify candidates that might mediate HH signaling. Here, we find that PLXNs from both the A and B subfamilies can promote HH signaling, which may be an important clue in answering this question. While we cannot exclude the possibility that each PLXN or PLXN subfamily regulates HH differently, it is likely that they converge upon a common

399 protein or set of proteins that mediate HH promotion. Our data suggest that this
400 convergence takes place at the level of GLI transcription factors and requires intact
401 primary cilia. Therefore, candidates for future study should have common demonstrated
402 roles downstream of all PLXNs.
403
404 *PLXN Redundancy in HH Pathway Promotion*
405 As previously discussed, the PLXN family of proteins is comprised of nine
406 members with distinct and overlapping functions (Neufeld and Kessler 2008). One shared
407 feature between all PLXN proteins is the conserved cytoplasmic GAP domain (Neufeld
408 and Kessler 2008), which we find mediates HH signal promotion. Therefore, our results
409 are complicated by the presence of endogenous PLXN proteins that may act redundantly
410 in the HH signaling cascade, particularly given that PLXNs from multiple subfamilies
411 promote HH signaling. Though technically challenging, a PLXN null background would
412 be necessary to truly study the function of individual PLXN family members in HH
413 signaling. It is also important to consider that PLXNs exhibit largely overlapping
414 expression patterns *in vivo*, further complicating loss-of-function studies (Perala et al.
415 2005; Mauti et al. 2006). Notably, our results suggest that deleting *Plxna1* or *Plxna2*
416 alone is sufficient to reduce HH target gene expression in the dentate gyrus (Figure 6),
417 despite the widespread expression of additional *Plxns* in the central nervous system
418 (Perala et al. 2005). Additional HH-responsive tissues that express a smaller subset of
419 *Plxns*, including the olfactory epithelium, the tooth bud, and the lung (Perala et al. 2005),
420 should be considered for broader *in vivo* studies.

Our study and many others highlight the complex, entangled nature of cell signaling molecules and pathways. While they are typically studied in isolation, it may be useful to instead consider signaling pathways as broader signaling networks, with overlapping inputs and outputs that combine to elicit cellular behaviors. By better understanding these systems, we can begin to decode the factors influencing cellular decision-making in developmental, homeostatic, and diseased states.

Materials and Methods

Plxn Constructs

Plxn constructs were derived from full length cDNAs using standard molecular biology techniques. All constructs were cloned into the *pCIG* vector, which contains a CMV enhancer, a chicken beta actin promoter, and an internal ribosome entry site (IRES) with a nuclear enhanced green fluorescent protein reporter (3XNLS-EGFP) (Megason and McMahon 2002). C-terminal or N-terminal 6X MYC tags (EQKLISEEDL) were added to constructs as indicated. Deletion and mutation variants were generated using standard cloning techniques and the QuickChange II XL Site-Directed Mutagenesis Kit (Agilent Technologies, 200521).

Cell Culture and MEF generation

Cell lines were maintained in Dulbecco's Modified Eagle Medium (DMEM; ThermoFisher Scientific, 11965-118) supplemented with 10% bovine calf serum (ATCC, 30-2030) and 1X Penicillin-Streptomycin-Glutamine (Life Technologies, 10378016).

443 Cultures were maintained at 37 °C with 5% CO_2 and 95% humidity. MEFs were
444 generated as previously described (Todaro and Green 1963).
445
446 *Cell Signaling Assays*
447 Luciferase-based reporter assays for HH pathway activity in NIH/3T3 cells were
448 performed as previously described using a ptcΔ136-GL3 reporter construct (Nybakken et
449 al. 2005). Briefly, cells were seeded at 2.5 X 10^4 cells/well into 0.5% gelatin-coated 24-
450 well plates. The next day, cells were transfected with empty vector (*pCIG*) or
451 experimental constructs along with the *ptcΔ136-GL3* luciferase reporter construct and
452 beta-galactosidase transfection control (pSV-β-galactosidase; Promega, E1081).
453 Transfections were performed using Lipofectamine 2000 (Invitrogen, 11668) and Opti-
454 MEM reduced serum media (Invitrogen, 31985). 48h after transfection, culture media
455 was replaced with low-serum media (0.5% bovine calf serum, 1% Penicillin
456 Streptomycin L-Glutamine) containing either control or N-terminal SHH (NSHH)-
457 conditioned media. Luciferase reporter activity and Beta Galactosidase activity were
458 measured 48h later on a Spectramax M5^e Plate reader (Molecular Devices) using the
459 Luciferase Assay System (Promega, E1501) and the Betafluor Beta Galactosidase Assay
460 Kit (EMD Millipore, 70979), respectively. Luciferase values were divided by beta
461 galactosidase activity to control for transfection, and data were reported as fold induction
462 relative to the vector-transfected control. All treatments were performed in triplicate
463 (each data point indicates a technical replicate) and averaged (bar height), with error bars
464 representing the standard deviation between triplicate wells. Each experiment was
465 repeated a minimum of three times (biological replicates); representative results are

466 shown. Student's t-tests were used to determine whether each treatment was significantly
467 different from the control, with P-values of 0.05 or less considered statistically
468 significant.
469
470 *Immunofluorescent Analyses for cultured cells*
471 NIH/3T3 fibroblasts were plated at 1.5 X 10^5 cells/well onto glass coverslips in a
472 6-well dish. Cells were transfected 24h after plating using Lipofectamine 2000
473 (Invitrogen, 11668) and Opti-MEM reduced serum media (Invitrogen, 31985). To assess
474 expression and collapse, cells were incubated for 24-48h at 37 °C as indicated. To image
475 cilia, cells were placed in low serum media approximately 6h after transfection (0.5%
476 bovine calf serum, 1% Penicillin Streptomycin L-Glutamine) for 48h. All cells were fixed
477 in 4% paraformaldehyde for 10min at room temperature and washed with PBS. A 5min
478 permeabilization step with 0.2% Triton X-100 in PBS was performed as indicated, prior
479 to staining. Primary antibodies included: mouse IgG2a anti-MYC (1:1000, Cell
480 Signaling, 2276), goat IgG anti-PLXNA1 (1:250, R&D Systems, AF4309), and mouse
481 IgG2b anti-acetylated tubulin (1:2500, Sigma Aldrich, T7451), all diluted in IF blocking
482 buffer (list reagents please – I don't have the recipe on hand!). Coverslips were incubated
483 with primary antibodies overnight, followed by a 10min DAPI stain (1:30,000 in PBS at
484 room temperature, Invitrogen, D1306) and 1h incubation with secondary antibodies
485 including: AlexaFluor 555 goat anti-mouse IgG2a, AlexaFluor 488 donkey anti-goat IgG,
486 AlexaFluor 488 goat anti-mouse IgG2b, and AlexaFluor 555 goat anti-mouse IgG2b
487 (1:500, Invitrogen, A21137, A11055, A21141, and A21147, respectively). Coverslips
488 were mounted to glass slides using Shandon Immu-Mount Mounting Medium (Fisher,

9990412). Immunofluorescent analysis and imaging were performed on a Leica SP5X Upright 2-Photon Confocal microscope using LAS AF software (Leica) and a Leica 63X (type: HC Plan Apochromat CS2; NA1.2) water immersion objective.

Western Blot Analysis

NIH/3T3 cells were transfected using Lipofectamine 2000 (Invitrogen, 11668) and Opti-MEM reduced serum media (Invitrogen, 31985). Cells were lysed in radioimmunoprecipitation assay (RIPA) buffer (50 mM Tris-HCl, pH 7.2, 150 mM NaCl, 0.1% Triton X-100, 1% sodium deoxycholate, and 5 mM EDTA) 48h after transfection, sonicated using a Fisher Scientific Sonic Dismembrator, Model 500 (4 pulses at 20%), and centrifuged at 14,000 x *g* for 25min at 4 °C to remove the insoluble fraction. Protein concentrations were determined using the BCA Protein Assay Kit (Fisher, PI23225). After boiling for 10min, 50µg of protein from each sample were separated using SDS-PAGE with 7.5-12.5% gels and transferred onto Immun-Blot PVDF membranes (Bio-Rad, 162-0177). Membranes were washed in tris-buffered saline (TBS) with 0.5% OmniPur Tween-20 (TBST; EMD Millipore, 9480) and blocked in western blocking buffer (30 g/L Bovine Serum Albumin with 0.2% NaN_3 in TBST) for 1h to overnight. Blots were probed with the following antibodies: rabbit IgG anti-MYC (1:10,000, Bethyl Labs, A190-105A), goat IgG anti-PLXNA1 (1:200, R&D Systems, AF4309), and Mouse IgG1 anti-Beta Tubulin (1:10,000, generously provided by Dr. Kristen J. Verhey, University of Michigan). Secondary antibodies from Jackson ImmunoResearch were diluted 1:10,000, and included: peroxidase-conjugated AffiniPure goat anti-mouse IgG, light chain specific (115-035-174), peroxidase-conjugated AffiniPure F(ab)2 Fragment

donkey anti-rabbit IgG (711-036-152), and peroxidase-conjugated AffiniPure donkey anti-goat IgG, light chain specific (705-035-147). Immobilon Western Chemiluminescent HRP Substrate (EMD Millipore, WBKLS0500) was added for 10min before membranes were exposed to HyBlot CL Audoradiography Film (Denville, E3018) and developed using a Konica Minolta SRX-101A Medical Film Processor.

RNAi

RNAi was performed using Lipofectamine RNAiMAX Transfection Reagent (ThermoFisher Scientific, 13778150) with BLOCK-iT Fluorescent Oligo as a transfection control (ThermoFisher Scientific, 13750062). *Plxn* knockdown was performed using Dharmacon ON-TARGET*plus* SMARTpool reagents with catalog numbers L-040789-01-0005, L-040790-01-0005, L-040791-01-0005, L-040980-00-0005, and L-056934-01-0005 for *Plxna1*, *Plxna2*, *Plxna3*, *Plxnb2*, and *Plxnd1*, respectively. *Nrp* oligos included *Nrp1*: GCACAAAUCUCUGAAACUA; and *Nrp2*: GACAAUGGCUGGACACCCA.

RT-qPCR

NIH/3T3 cells were cultured as previously described and treated with low-serum media (0.5% bovine calf serum, 1% Penicillin Streptomycin L-Glutamine) containing SAG as indicated. RNA was isolated using the RNAqueous kit (ThermoFisher Scientific, AM1912). cDNA was generated using 1 μg of template RNA (iScript RT Supermix, BioRad, 1708841). cDNA was diluted 1:100, and qPCR was performed using SYBR green master mix (ThermoFisher Scientific, AM9780) on an Applied BioSystems StepOnePlus Real-Time PCR System with the following primers: *Gli1* forward:

GTGCACGTTTGAAGGCTGTC; *Gli1* reverse: GAGTGGGTCCGATTCTGGTG; *Ptch1* forward: GAAGCCACAGAAAACCCTGTC; *Ptch1* reverse: GCCGCAAGCCTTCTCTAGG; *Cyclophilin* forward: TCACAGAATTATTCCAGGATTCATG; and *Cyclophilin* reverse: TGCCGCCAGTGCCATT. *Cyclophilin* expression was used for normalization.

Chicken in ovo Neural Tube Electroporation

Electroporations were performed as previously described (Tenzen et al. 2006), using *Plxn*, *SmoM2*, and *Gli1* constructs cloned into the pCIG vector (Megason and McMahon 2002). Briefly, DNA constructs (1.0 μg/μl) were mixed with 50 ng/μl Fast green FCF dye (Millipore Sigma, F7252) and injected into the neural tube of Hamburger Hamilton stage 11-13 chicken embryos (Hamburger and Hamilton 1951). Embryos were dissected 48-hours post-injection and screened for GFP expression before being fixed in 4% PFA and prepared for immunofluorescent analysis. Embryos were embedded in Tissue-Tek OCT compound (Thermo Fisher Scientific, NC9806257), rapidly frozen over dry ice, and cryo-sectioned at a thickness of using a Leica cryostat. Twelve micron thick samples were affixed to glass slides and immunostained using the following antibodies: mouse IgG1 anti-PAX7 (1:20, Developmental Studies Hybridoma Bank, DSHB), mouse IgG1 anti-NKX6.1 (1:20, DSHB), goat IgG anti-GFP (1:200, Abcam, ab6673), rabbit IgG anti-MYC (1:100, Bethyl Laboratories, A190-205A). Slides were incubated with primary antibody overnight at 4˚C followed by a 10min DAPI stain (1:30,000 at room temperature, Invitrogen, D1306) and 1h incubation with secondary antibodies including: AlexaFluor 555 donkey anti-mouse IgG, AlexaFlour 488 donkey anti-goat IgG,

AlexaFlour 647 donkey anti-rabbit IgG (1:500, Invitrogen, A31570, A11055, A31573, respectively). Samples were visualized on a Leica Upright SP5X Light Laser Confocal Microscope, and figures were generated using Adobe Photoshop and Illustrator. The size of the NKX6.1 domain was measured using Adobe Illustrator in chicken neural tubes electroporated with *pCIG* (n=6), *Gli1* (n=4), and *Plxna1*$^{\Delta ECD}$ (n=17). These measurements were then normalized to the NKX6.1 domain size of the unelectroporated side of the neural tube.

Mice

Plxna1 (Yoshida et al. 2006) and *Plxna2* (Suto et al. 2007; Duan et al. 2014) mice, both on mixed genetic backgrounds, were generously provided by Dr. Alex Kolodkin. *Gli1*^{lacZ} animals were maintained on a mixed CD1 and C57BL/6J background (Bai et al. 2002). All mice were housed and cared for according to NIH guidelines, and all animal research was approved by the University of Michigan Medical School Institutional Animal Care and Use Committee. *Plxn* genotyping was performed using the following primers: *Plxna1* WT_F: CCTGCAGATTGATGACGACTTCTG; *Plxna1* WT_R: TCATGAGACCCAGTCTCCCTGTC; *Plxna1* MT_F: GCATGCCTGTGACACTTGGCTCACT; *Plxna1* MT_R: CCATTGCTCAGCGGTGCTGTCCATC; *Plxna2* WT_F: GCTGGAACCATGTGAGAGCTGATC; *Plxna2* WT_R; GGTCATCTAGTCGCAGGAGCTTGC; *Plxna2* MT_F: GGTCATCTAGTCGCAGGAGCTTGC; *Plxna2* MT_R: TACCCGTGATATTGCTGAAGAGCTTGG. Tissue preparation and X-gal staining

were performed as previously described (Duan et al. 2014; Holtz et al. 2015). Briefly, serial sagittal sections (16μm) were collected from P7 brains and mounted onto six slides. One slide from each animal was used for X-gal staining. The total number of X-gal positive cells was quantified from eight serial sections per slide to yield the average number of X-gal positive cells per animal; each data point represents a single animal.

Acknowledgements

We are grateful to Dr. A. L. Kolodkin (Johns Hopkins University, MD, USA) for providing *Plxn* constructs. Members of the Allen and Giger labs contributed technical assistance, insightful comments, and helpful suggestions. We are also thankful to Drs. K. S. O'Shea, K. J. Verhey, and J. D. Engel for sharing equipment and reagents. Confocal imaging was performed in the Microscopy Core at the University of Michigan. We acknowledge the ENCODE consortium, and particularly the lab of Dr. John Stamatoyannopoulous at the University of Washington for sharing their RNA-seq dataset on NIH/3T3 cells (GEO: GSM970853). J.M.P. was supported by a Rackham Merit Fellowship, Benard Maas Fellowship, Bradley Merrill Patten Fellowship, Organogenesis Training Grant (T32 HD007505), and Ruth L. Kirschstein National Research Service Award (F31 NS096734). R.J.G. is supported by the Adelson Medical Foundation, Craig H. Neilsen Foundation, and funding from the National Institutes of Health (R01 MH119346). B.L.A. is supported by funding from the National Institutes of Health (R01 DC014428, R01 CA198074 and R01 GM118751). B.L.A. and R.J.G. are supported by an MCubed Research Grant from The University of Michigan.

Author Contributions

J.M. Pinskey: Conceptualization, Validation, Formal Analysis, Investigation, Writing- Original Draft, Writing- Review & Editing. T.M. Hoard: Conceptualization, Validation, Formal Analysis, Investigation, Writing- Original Draft, Writing- Review & Editing. X-F Zhao: Formal Analysis, Investigation. N.E. Franks: Formal Analysis, Investigation. Z.C. Frank: Investigation. A.N. McMellen: Investigation. R.J. Giger: Conceptualization, Resources, Formal Analysis, Investigation, Writing- Original Draft, Writing- Review and Editing. B.L. Allen: Conceptualization, Resources, Formal Analysis, Supervision, Funding Acquisition, Investigation, Methodology, Project Administration, Writing- Original Draft, Writing- Review and Editing.

Pinskey and Hoard et al., 2021, Figure 1

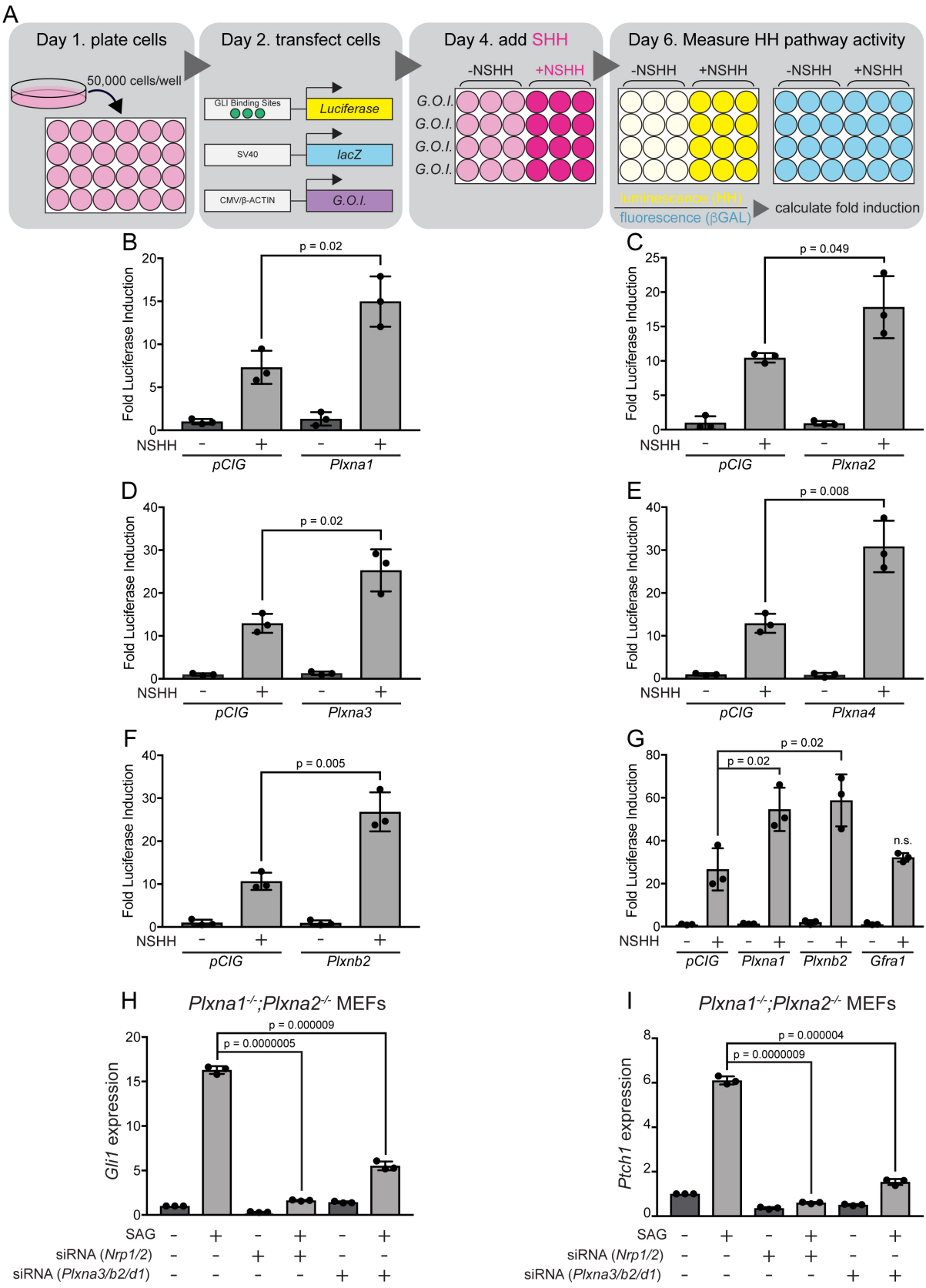

Figure 1. Multiple PLXNs promote HH signaling.

(A) Schematic of HH-responsive NIH/3T3 luciferase assays. G.O.I, gene of interest. (B-F) HH-dependent luciferase reporter activity was measured in NIH/3T3 cells transfected with the indicated constructs and stimulated with control (-NSHH) or NSHH-conditioned media (+NSHH). (G) Direct analysis of PLXNA1- and PLXNB2-mediated HH pathway promotion, compared with the unrelated cell surface protein GFRα1. (H-I) qRT-PCR analysis of *Gli1* and *Ptch1* in response to HH pathway activation via the Smoothened agonist, SAG. *Plxna1*$^{-/-}$;*Plxna2*$^{-/-}$ MEFs were treated with siRNA oligos for either *Nrp1* and *Nrp2* or *Plxna3, Plxnb2,* and *Plxnd1,* as indicated. Data points indicate technical replicates. Fold changes were determined using the ΔΔCT method. Data are reported as mean fold induction ± S.D., with p-values calculated using two-tailed Student's t tests. n.s. = not significant.

Figure 1- Source Data 1

Raw Data for Figure 1B-I

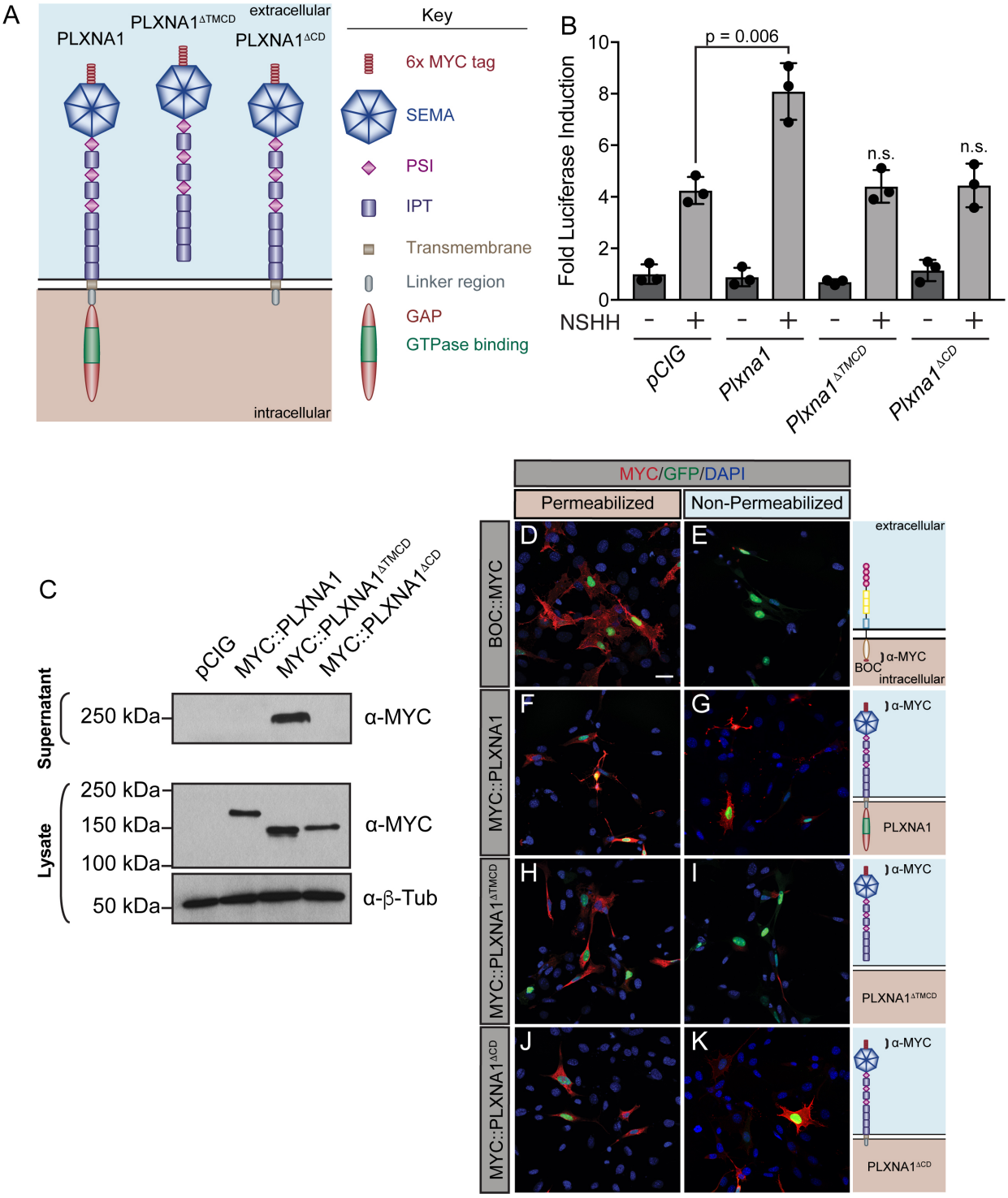

631 **Figure 2. The PLXNA1 cytoplasmic and transmembrane domains are required for**
632 **HH pathway promotion.** (A) Schematic of different PLXNA1 proteins. (B) HH-
633 dependent luciferase reporter activity was measured in NIH/3T3 cells transfected with the
634 indicated constructs and stimulated with control (-NSHH) or NSHH-conditioned media
635 (+NSHH). Data are reported as mean fold induction ± S.D. with p-values calculated using
636 two-tailed Student's t tests. n.s. = not significant. (C) Western blot analysis confirming
637 expression of MYC-tagged PLXNA1 proteins in NIH/3T3 cells. Note that
638 MYC::PLXNA1$^{\Delta TMCD}$ is detected in the supernatant, consistent with its predicted
639 secretion. Anti-Beta-tubulin (α-β-Tub) was used as a loading control. (D-K) Antibody
640 detection of MYC (red) in permeabilized (left panels) and non-permeabilized (right
641 panels) NIH/3T3 cells to assess cell surface localization of the indicated MYC-tagged
642 proteins. Note that BOC, which contains a C-terminal MYC tag is only detected under
643 permeabilized conditions, while PLXNA1$^{\Delta TMCD}$, which is secreted, is also largely
644 undetected under non-permeabilized conditions. Nuclear GFP (green) indicates
645 transfected cells, whereas DAPI (blue) stains all nuclei. Diagrams (right) describe each
646 construct, with brackets indicating antibody binding sites. Scale bar = 10μm.
647
648 **Figure 2- Source Data 1**
649 Raw data for Figure 2B
650 **Figure 2- Source Data 2**
651 Raw, unedited blot from Figure 2C
652 **Figure 2- Source Data 3**
653 Raw, unedited blot from Figure 2C

654 **Figure 2- Source Data 4**

655 Raw, unedited blot from Figure 2C

656 **Figure 2- Source Data 5**

657 Raw, labeled blot from Figure 2C

658 **Figure 2- Source Data 6**

659 Raw, labeled blot from Figure 2C

660 **Figure 2- Source Data 7**

661 Raw, labeled blot from Figure 2C

Pinskey and Hoard et al., 2021, Figure 3

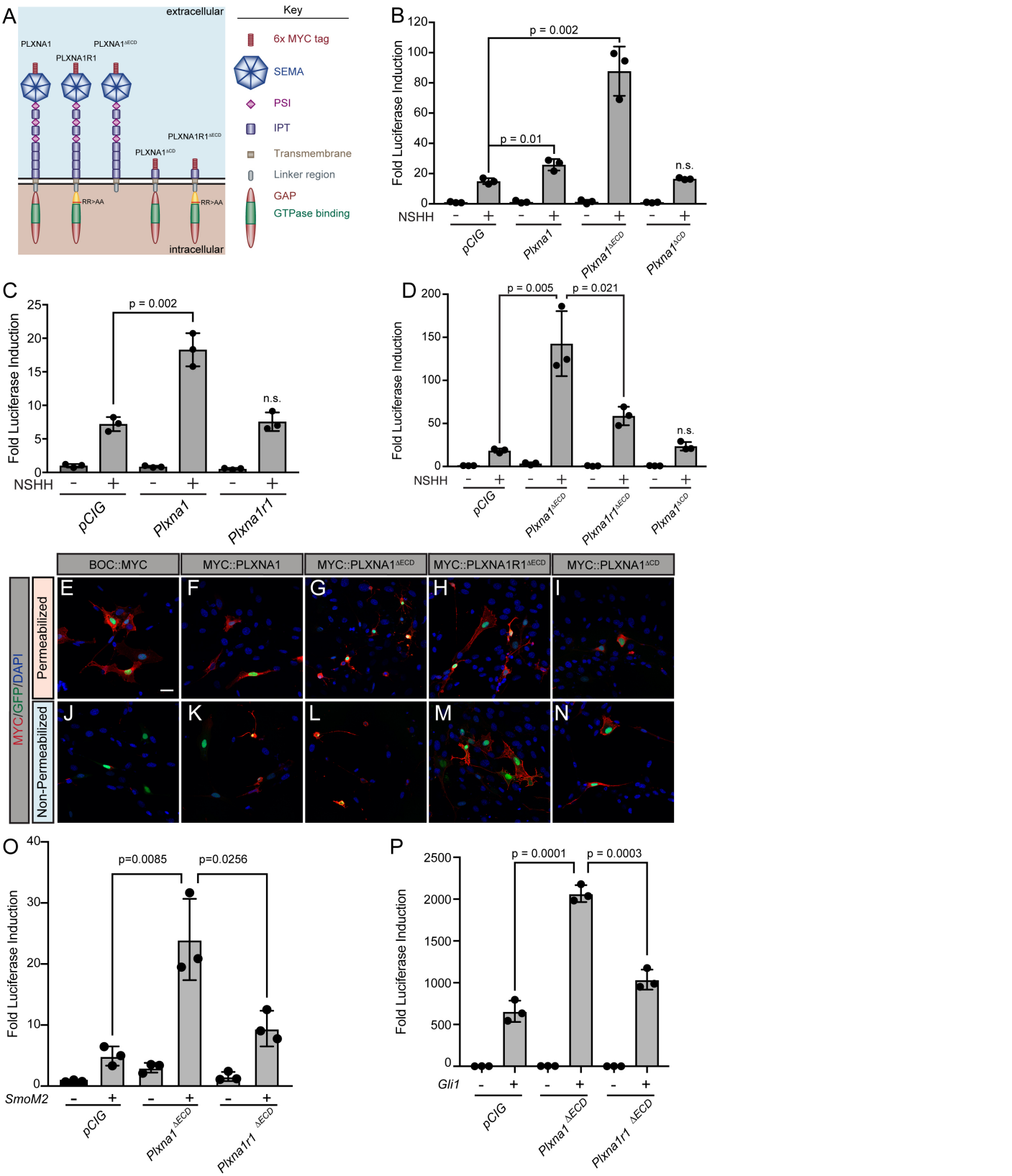

Figure 3. The Plexin GAP domain is required to promote Hedgehog signaling at the level of GLI transcription factors. (A) Schematic of different PLXNA1 proteins. (B-D) HH-dependent luciferase reporter activity was measured in NIH/3T3 cells transfected with the indicated constructs and stimulated with control (-NSHH) or NSHH-conditioned media (+NSHH). Data are reported as mean fold induction ± S.D. with p-values calculated using two-tailed Student's t tests. n.s. = not significant. (E-N) Antibody detection of MYC-tagged proteins (red) in permeabilized (top panels) and non-permeabilized (bottom panels) NIH/3T3 cells to assess cell surface localization of the indicated constructs. Nuclear GFP (green) indicates transfected cells, whereas DAPI (blue) stains all nuclei. Note that constitutive PLXN GAP activity leads to cell collapse, as is observed with PLXNA1$^{\Delta ECD}$ and, to some extent, PLXNA1. For PLXNA1R1 localization, please see Figure S2, D-E. Scale bar = 10 μm. (O-P) HH-dependent luciferase reporter activity was measured in NIH/3T3 cells transfected with the indicated constructs and stimulated by co-transfecting cells with *pCIG*, *SmoM2* (O), or *Gli1* (P). Data are reported as mean fold induction ± S.D., with p-values calculated using two-tailed Student's t tests. n.s. = not significant.

Figure 3- Source Data 1

Raw data for Figure 3B-D and Figure 3O-P

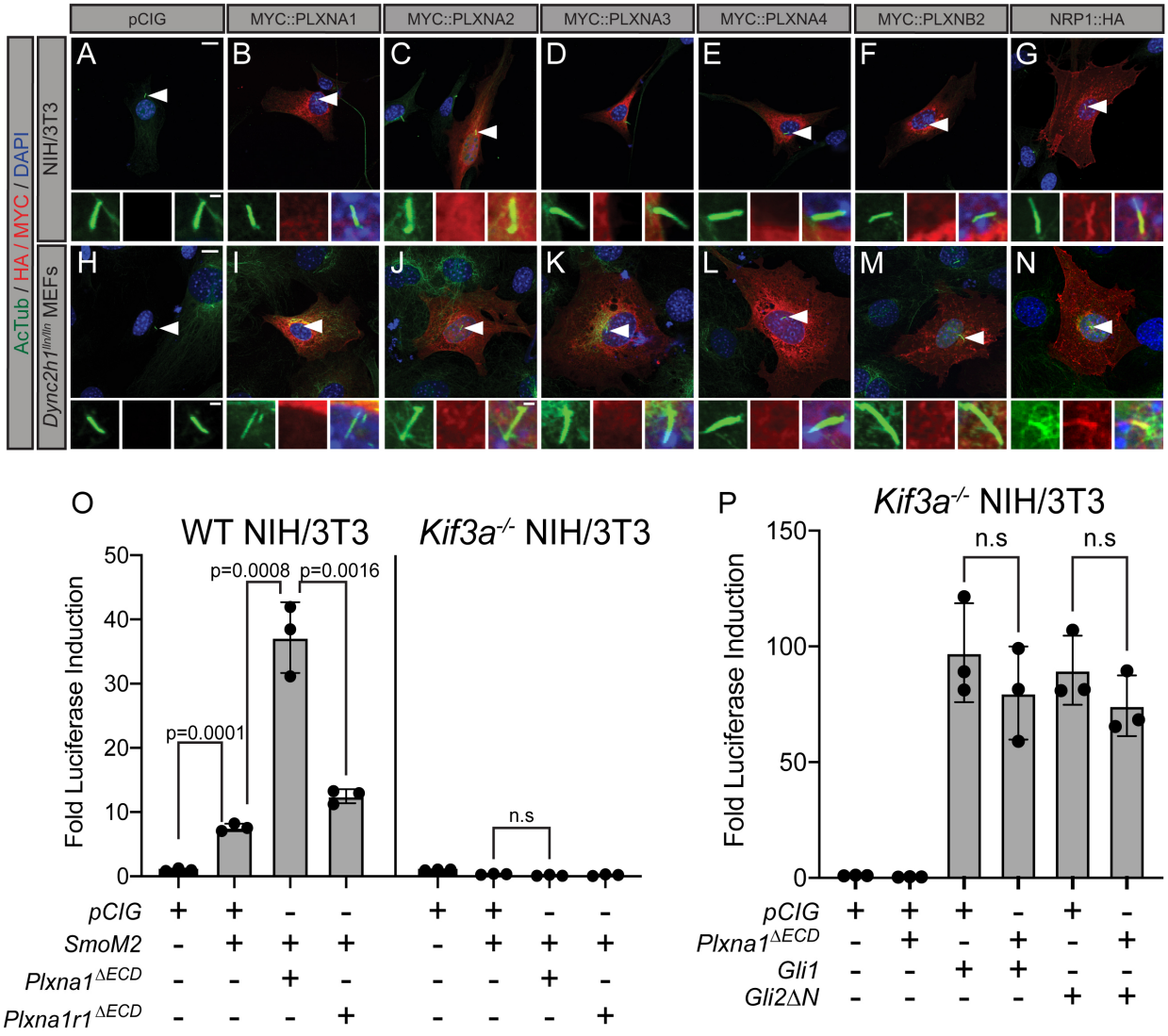

683 **Figure 4. PLXNs do not localize to primary cilia, but do require primary cilia to**
684 **promote HH pathway activity.** (A-N) Antibody detection of MYC and HA tagged
685 constructs (red) in NIH/3T3 cells (A-G) and *Dync2h1*$^{lln/lln}$ MEFs (H-N). Acetylated
686 tubulin (AcTub, green) indicates the primary cilium and DAPI (blue) stains nuclei.
687 Compared to NRP1, PLXNs are not enriched in primary cilia. Scale bar = 10 μm. Inset
688 scale bar = 1 μm. (O) WT NIH/3T3 cells or *Kif3a*$^{-/-}$ NIH/3T3 cells were co-transfected
689 with *SmoM2* and *Plxna1*$^{\Delta ECD}$ or *Plxna1r1*$^{\Delta ECD}$. (P) *Kif3a*$^{-/-}$ NIH/3T3 were transfected with
690 *Gli1* or *Gli2ΔN* and co-transfected with *Plxna1*$^{\Delta ECD}$. Data are reported as mean fold
691 induction ± S.D., with p-values calculated using two-tailed Student's t tests. n.s. = not
692 significant.
693
694 **Figure 4- Source Data 1**
695 Raw data for Figure 4 O-P

Pinskey and Hoard et al., 2021, Figure 5

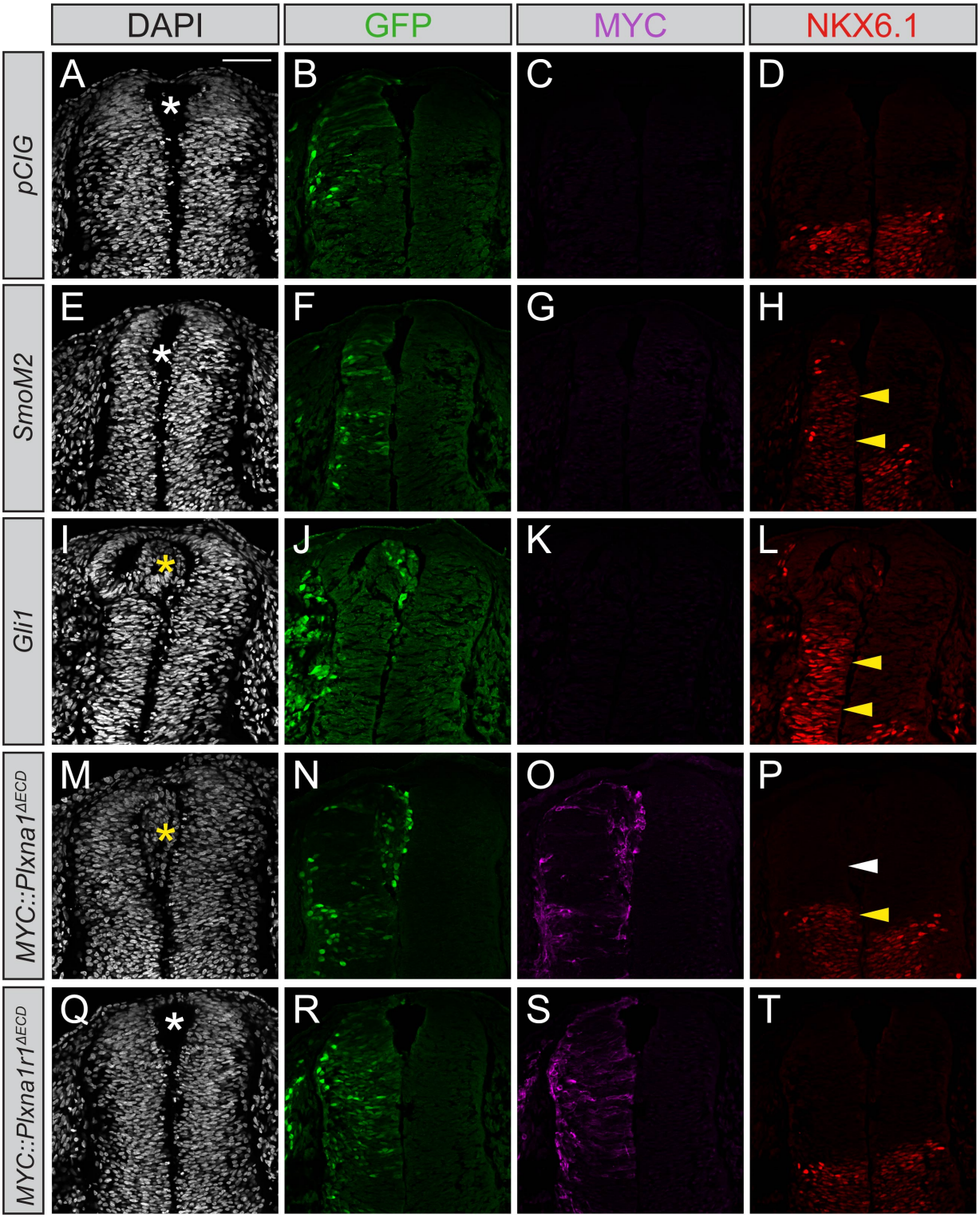

Figure 5. Constitutively active PLXNA1 induces ectopic cell migration into the lumen of the developing chicken neural tube. (A-T) Immunofluorescent analysis of neural patterning in forelimb-level sections from Hamburger-Hamilton stage 21-22 chicken embryos. Embryos were electroporated at Hamburger-Hamilton stage 11-13 with *pCIG* (A-D, n= 6 embryos), *SmoM2* (E-H, n = 7 embryos), *Gli1* (I-L, n = 4 embryos), *MYC::Plxna1*$^{\Delta ECD}$ (M-P, n = 17 embryos), or *MYC::Plxna1r1*$^{\Delta ECD}$ (Q-T, n = 6 embryos). Transverse sections were stained with GFP, MYC, and NKX6.1 antibodies. DAPI stain labels nuclei (gray). Electroporated cells are labeled with GFP. Asterisks denote the presence (yellow) or absence (white) of ectopic cells within the lumen of the neural tube. Arrowheads denote the presence (yellow) or absence (white) of ectopic NKX6.1. Scale bar = 50 μm.

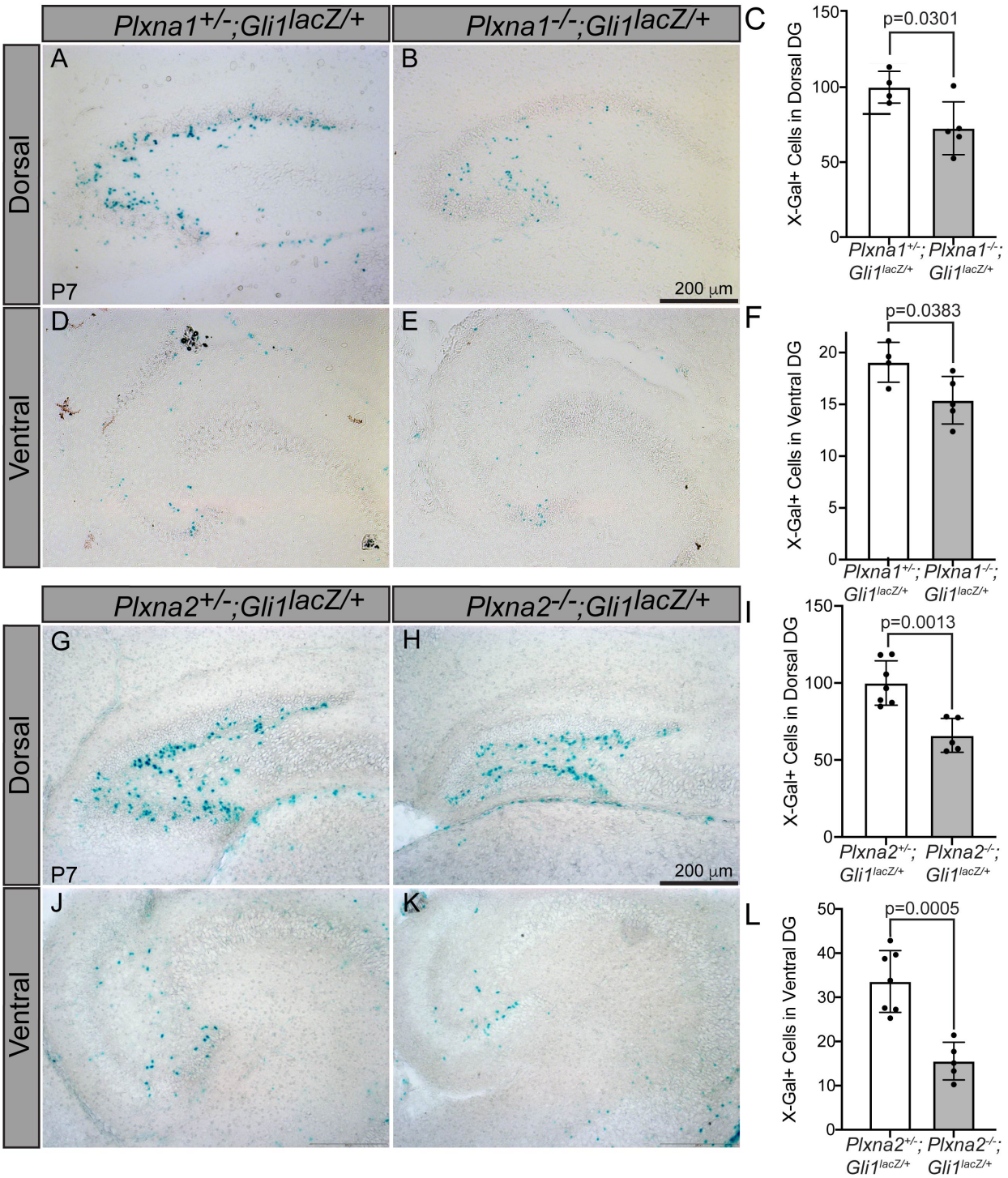

Figure 6. Reduced *Gli1*^{lacZ} expression in the dentate gyrus of mice lacking either *Plxna1* or *Plxna2*. X-Gal staining in coronal sections through the dorsal (A, B, G, and H) and ventral (D, E, J, and K) hippocampus of postnatal day 7 (P7) mice. The following numbers of pups were analyzed: *Plxna1*$^{+/-}$;*Gli1*$^{lacZ/+}$ (n=4); *Plxna1*$^{-/-}$;*Gli1*$^{lacZ/+}$ (n=5); *Plxna2*$^{+/-}$;*Gli1*$^{lacZ/+}$ (n=7); *Plxna2*$^{-/-}$;*Gli1*$^{lacZ/+}$ (n=5). Quantitation of *Gli1*^{lacZ} positive cells (C, F, I, and L) reported as mean ± S.D. with p-values calculated using two-tailed Student's t test. DG = dentate gyrus. Scale bar = 200 μm.

Figure 6- Source Data 1

Raw data for Figure 6C, F, I, L

Pinskey and Hoard et al., 2021, Figure 7

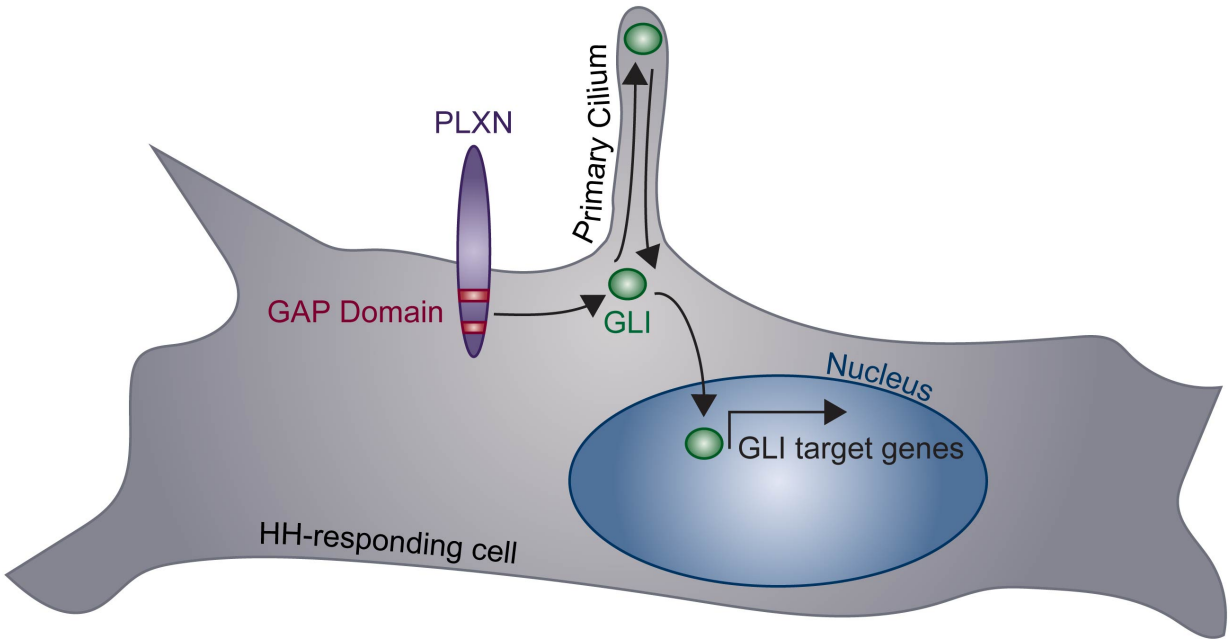

Figure 7. Model of PLXN-mediated promotion of HH pathway activity.

PLXNs (purple) at the cell surface promote HH signaling through GLI transcription factor (green) activation, mediated by their cytoplasmic GAP activity (red). Notably, this PLXN-dependent promotion requires primary cilia to induce GLI target gene expression in the nucleus.

Pinskey and Hoard et. al., 2021, Figure S1

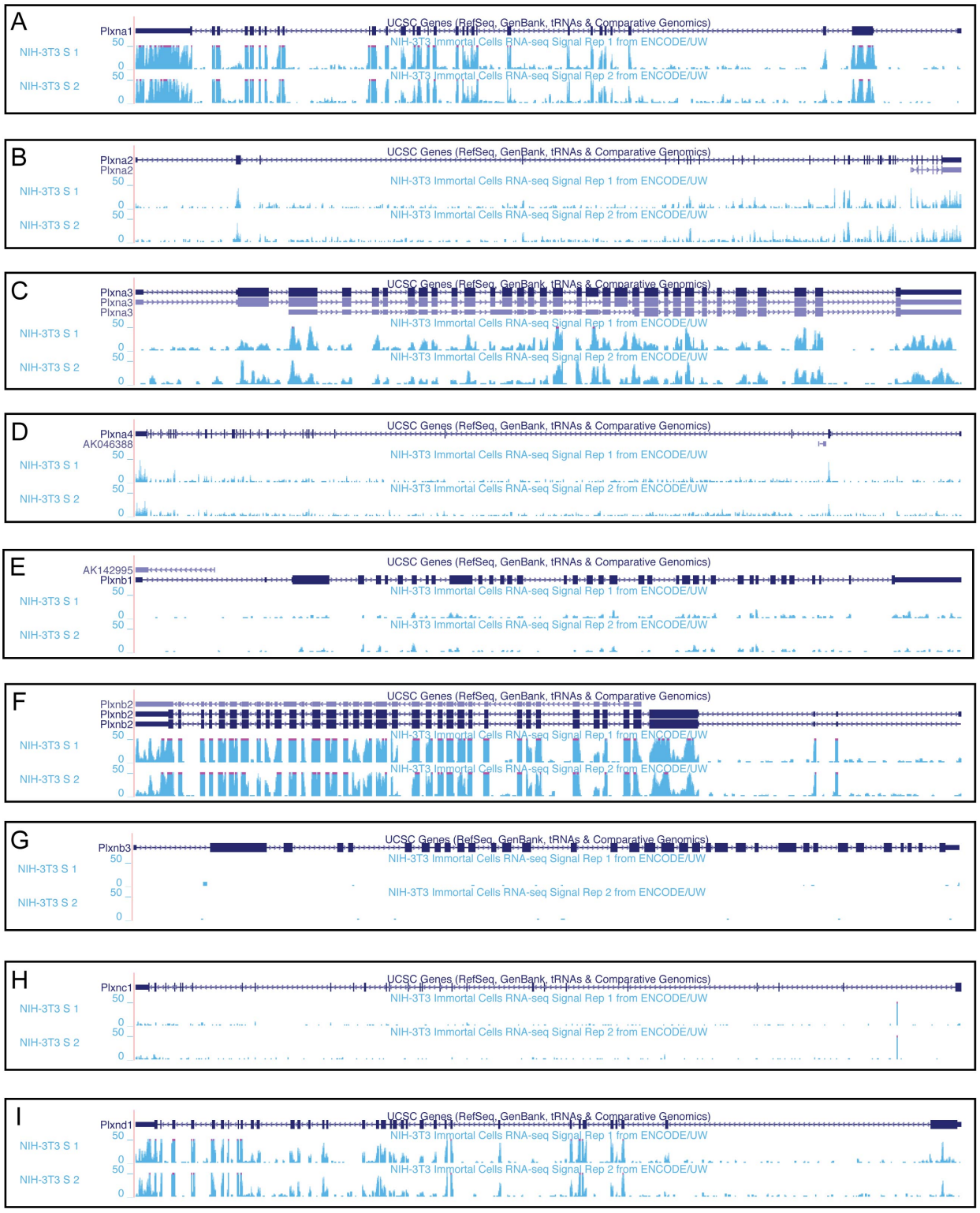

Figure S1. *Plxn* expression in NIH/3T3 fibroblasts.

RNA sequencing data from the ENCODE project indicating *Plxn* expression in NIH/3T3 cells. Data were aligned to the mouse GRCm38/mm10 assembly using the UCSC Genome Browser (https://genome.ucsc.edu).

A

assay	PLXNA1 fold change	PLXNA1 p-value	PLXNA1$^{\Delta ECD}$ fold change	PLXNA1$^{\Delta ECD}$ p-value
1	1.63	0.024	6.85	0.0004
2	1.50	0.047	3.69	0.00001
3	1.33	0.036	4.80	0.007
4	1.77	0.056	10.42	0.00005
5	1.72	0.011	5.85	0.002
avg.	1.59	0.035	6.32	0.001

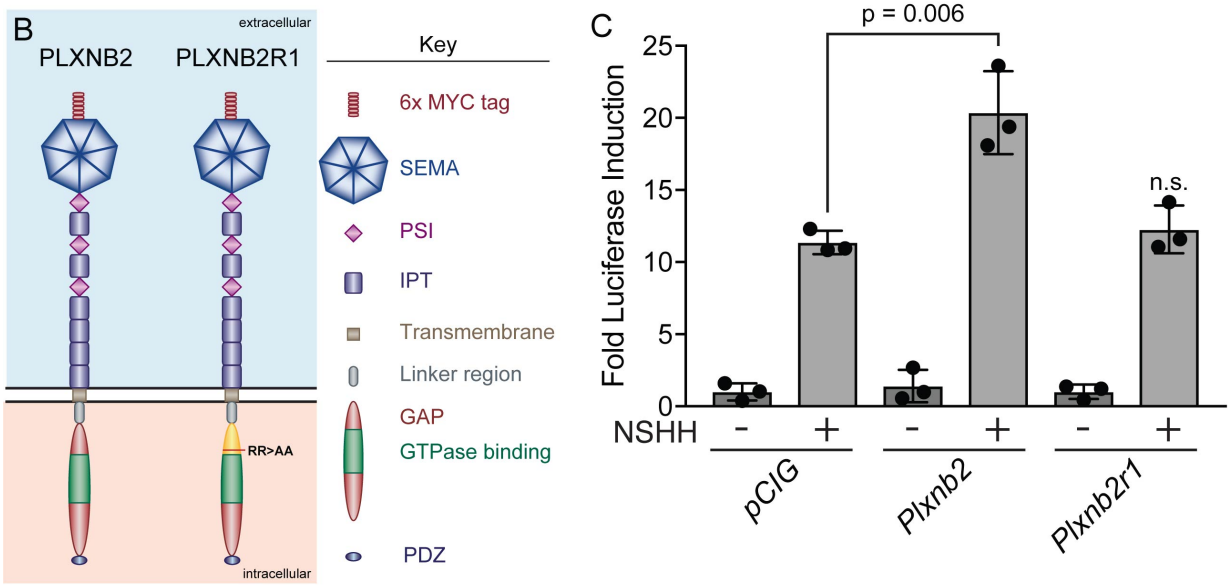

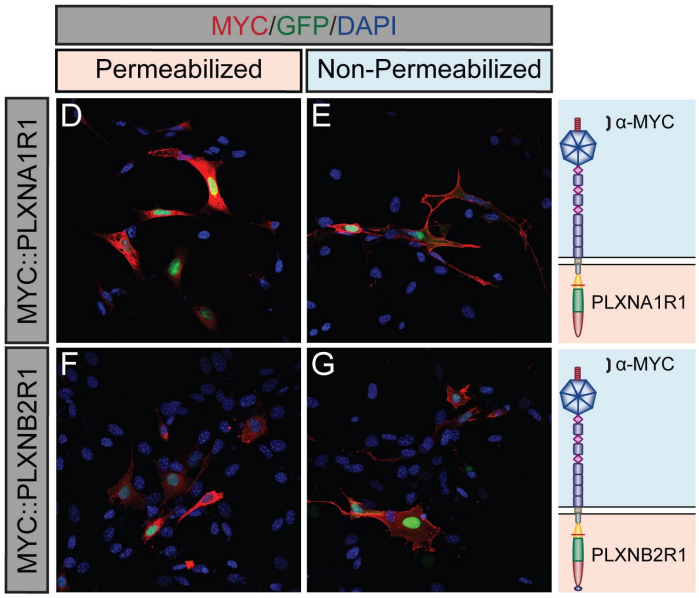

Figure S2. Constitutively active PLXNA1 reproducibly increases HH pathway activity. (A) Summary of luciferase assay data in which PLXNA1 and PLXNA1$^{\Delta ECD}$ were directly compared in five independent assays. Fold change reported between ligand-stimulated vector only (*pCIG*) triplicate wells and ligand-stimulated *Plxna1*- or *Plxna1*$^{\Delta ECD}$ - transfected triplicate wells. Yellow highlight denotes statistical significance ($p<0.05$). (B) Schematic of different PLXNB2 proteins. (C) HH-dependent luciferase reporter activity was measured in NIH/3T3 cells transfected with the indicated constructs and stimulated with control (-NSHH) or NSHH-conditioned media (+NSHH). Data are reported as mean fold induction ± S.D. with p-values calculated using two-tailed Student's t tests. n.s. = not significant. (D-G) Antibody detection of MYC (red) in permeabilized (left panels) and non-permeabilized (right panels) NIH/3T3 cells to assess cell surface localization of the indicated MYC-tagged proteins. Nuclear GFP (green) indicates transfected cells, whereas DAPI (blue) stains all nuclei. Diagrams (right) describe each construct, with brackets indicating antibody binding sites. Scale bar = 10μm.

Figure S2- Source Data 1

Raw data for Figure S2C

Pinskey and Hoard et al., 2021, Figure S3

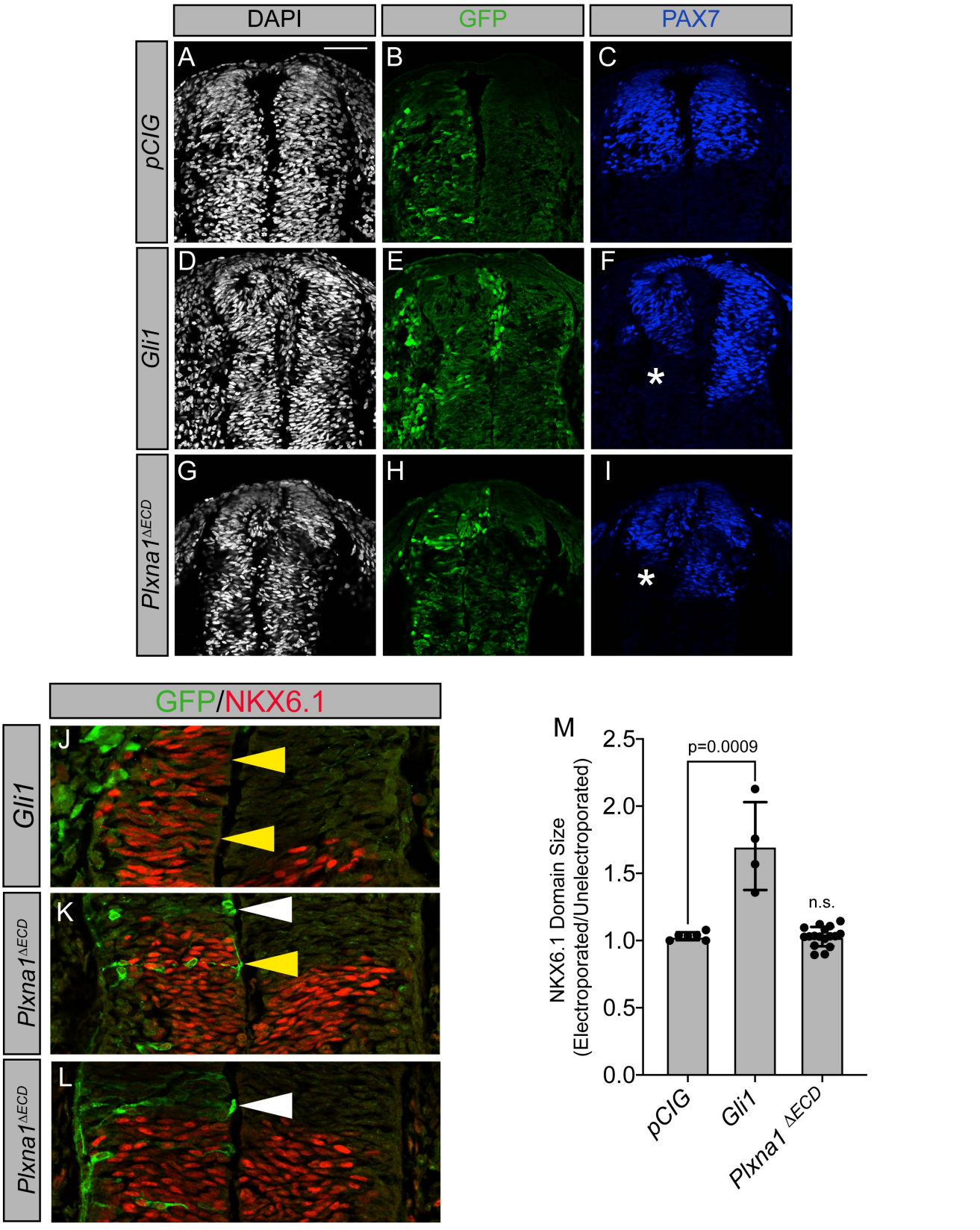

Figure S3. Constitutively active PLXNA1 does not significantly alter Hedgehog-dependent neural tube patterning in the developing chicken embryo. (A-M) Immunofluorescent analysis of neural patterning in forelimb level sections from Hamburger-Hamilton stage 21-22 chicken embryos. Embryos were electroporated at Hamburger-Hamilton stage 11-13 with *pCIG* (A-C), *Gli1* (D-F, J), or *Plxna1*$^{\Delta ECD}$ (G-I, K-L). Transverse sections were stained with antibodies directed against GFP (green), PAX7 (blue), and NKX6.1 (red). DAPI stain labels nuclei (gray). Electroporated cells are labeled with GFP. Asterisks denote the loss of PAX7. Scale bar = 50 μm. Yellow arrowheads indicate the presence of ectopic NKX6.1. White arrowheads (K-L) denote the absence of ectopic NKX6.1 in *Plxna1*$^{\Delta ECD}$-electroporated embryos as compared to *Gli1* (J). Quantitation of NKX6.1 domain size normalizing electroporated and unelectroporated sides of developing chicken neural tubes electroporated with *pCIG*, *Gli1*, or *PlxnA1*$^{\Delta ECD}$. Values are reported as mean ± S.D. with p-values calculated using two-tailed Student's t-test.

Figure S3- Source Data 1

Raw data for Figure S3M

References

Ahn S, Joyner AL. 2005. In vivo analysis of quiescent adult neural stem cells responding to Sonic hedgehog. *Nature* **437**: 894-897.

Alcedo J, Ayzenzon M, Von Ohlen T, Noll M, Hooper JE. 1996. The Drosophila smoothened gene encodes a seven-pass membrane protein, a putative receptor for the hedgehog signal. *Cell* **86**: 221-232.

Allen BL, Song JY, Izzi L, Althaus IW, Kang JS, Charron F, Krauss RS, McMahon AP. 2011. Overlapping roles and collective requirement for the coreceptors GAS1, CDO, and BOC in SHH pathway function. *Dev Cell* **20**: 775-787.

Allen BL, Tenzen T, McMahon AP. 2007. The Hedgehog-binding proteins Gas1 and Cdo cooperate to positively regulate Shh signaling during mouse development. *Genes Dev* **21**: 1244-1257.

Andreyeva T, Chaloupka FJ, Brownell KD. 2011. Estimating the potential of taxes on sugar-sweetened beverages to reduce consumption and generate revenue. *Prev Med* **52**: 413-416.

Bai CB, Auerbach W, Lee JS, Stephen D, Joyner AL. 2002. Gli2, but not Gli1, is required for initial Shh signaling and ectopic activation of the Shh pathway. *Development* **129**: 4753-4761.

Bandari S, Exner S, Ortmann C, Bachvarova V, Vortkamp A, Grobe K. 2015. Sweet on Hedgehogs: regulatory roles of heparan sulfate proteoglycans in Hedgehog-dependent cell proliferation and differentiation. *Curr Protein Pept Sci* **16**: 66-76.

Barberis D, Artigiani S, Casazza A, Corso S, Giordano S, Love CA, Jones EY, Comoglio PM, Tamagnone L. 2004. Plexin signaling hampers integrin-based adhesion, leading to Rho-kinase independent cell rounding, and inhibiting lamellipodia extension and cell motility. *Faseb J* **18**: 592-594.

Beachy PA, Hymowitz SG, Lazarus RA, Leahy DJ, Siebold C. 2010. Interactions between Hedgehog proteins and their binding partners come into view. *Genes Dev* **24**: 2001-2012.

Briscoe J, Therond PP. 2013. The mechanisms of Hedgehog signalling and its roles in development and disease. *Nat Rev Mol Cell Biol* **14**: 416-429.

Burke R, Nellen D, Bellotto M, Hafen E, Senti KA, Dickson BJ, Basler K. 1999. Dispatched, a novel sterol-sensing domain protein dedicated to the release of cholesterol-modified hedgehog from signaling cells. *Cell* **99**: 803-815.

Capurro MI, Xu P, Shi W, Li F, Jia A, Filmus J. 2008. Glypican-3 inhibits Hedgehog signaling during development by competing with patched for Hedgehog binding. *Dev Cell* **14**: 700-711.

Caspary T, Garcia-Garcia MJ, Huangfu D, Eggenschwiler JT, Wyler MR, Rakeman AS, Alcorn HL, Anderson KV. 2002. Mouse Dispatched homolog1 is required for long-range, but not juxtacrine, Hh signaling. *Curr Biol* **12**: 1628-1632.

Cayuso J, Marti E. 2005. Morphogens in motion: growth control of the neural tube. *J Neurobiol* **64**: 376-387.

Cayuso J, Ulloa F, Cox B, Briscoe J, Marti E. 2006. The Sonic hedgehog pathway independently controls the patterning, proliferation and survival of neuroepithelial cells by regulating Gli activity. *Development* **133**: 517-528.

Chang SC, Mulloy B, Magee AI, Couchman JR. 2011. Two distinct sites in sonic Hedgehog combine for heparan sulfate interactions and cell signaling functions. *J Biol Chem* **286**: 44391-44402.

Chen H, Chedotal A, He Z, Goodman CS, Tessier-Lavigne M. 1997. Neuropilin-2, a novel member of the neuropilin family, is a high affinity receptor for the semaphorins Sema E and Sema IV but not Sema III. *Neuron* **19**: 547-559.

Cheng HJ, Bagri A, Yaron A, Stein E, Pleasure SJ, Tessier-Lavigne M. 2001. Plexin-A3 mediates semaphorin signaling and regulates the development of hippocampal axonal projections. *Neuron* **32**: 249-263.

Christ A, Christa A, Klippert J, Eule JC, Bachmann S, Wallace VA, Hammes A, Willnow TE. 2015. LRP2 Acts as SHH Clearance Receptor to Protect the Retinal Margin from Mitogenic Stimuli. *Dev Cell* **35**: 36-48.

Christ A, Christa A, Kur E, Lioubinski O, Bachmann S, Willnow TE, Hammes A. 2012. LRP2 is an auxiliary SHH receptor required to condition the forebrain ventral midline for inductive signals. *Dev Cell* **22**: 268-278.

Conrotto P, Corso S, Gamberini S, Comoglio PM, Giordano S. 2004. Interplay between scatter factor receptors and B plexins controls invasive growth. *Oncogene* **23**: 5131-5137.

Consortium EP. 2012. An integrated encyclopedia of DNA elements in the human genome. *Nature* **489**: 57-74.

Corbit KC, Aanstad P, Singla V, Norman AR, Stainier DY, Reiter JF. 2005. Vertebrate Smoothened functions at the primary cilium. *Nature* **437**: 1018-1021.

Creanga A, Glenn TD, Mann RK, Saunders AM, Talbot WS, Beachy PA. 2012. Scube/You activity mediates release of dually lipid-modified Hedgehog signal in soluble form. *Genes Dev* **26**: 1312-1325.

Davis CA, Hitz BC, Sloan CA, Chan ET, Davidson JM, Gabdank I, Hilton JA, Jain K, Baymuradov UK, Narayanan AK et al. 2018. The Encyclopedia of DNA elements (ENCODE): data portal update. *Nucleic Acids Res* **46**: D794-D801.

Dessaud E, McMahon AP, Briscoe J. 2008. Pattern formation in the vertebrate neural tube: a sonic hedgehog morphogen-regulated transcriptional network. *Development* **135**: 2489-2503.

Duan Y, Wang SH, Song J, Mironova Y, Ming GL, Kolodkin AL, Giger RJ. 2014. Semaphorin 5A inhibits synaptogenesis in early postnatal- and adult-born hippocampal dentate granule cells. *Elife* **3**.

Engelke MF, Waas B, Kearns SE, Suber A, Boss A, Allen BL, Verhey KJ. 2019. Acute Inhibition of Heterotrimeric Kinesin-2 Function Reveals Mechanisms of Intraflagellar Transport in Mammalian Cilia. *Curr Biol* **29**: 1137-1148 e1134.

Fantin A, Schwarz Q, Davidson K, Normando EM, Denti L, Ruhrberg C. 2011. The cytoplasmic domain of neuropilin 1 is dispensable for angiogenesis, but promotes the spatial separation of retinal arteries and veins. *Development* **138**: 4185-4191.

Fard D, Tamagnone L. 2021. Semaphorins in health and disease. *Cytokine Growth Factor Rev* **57**: 55-63.

Ge X, Milenkovic L, Suyama K, Hartl T, Purzner T, Winans A, Meyer T, Scott MP. 2015. Phosphodiesterase 4D acts downstream of Neuropilin to control Hedgehog signal transduction and the growth of medulloblastoma. *Elife* **4**.

856 Giordano S, Corso S, Conrotto P, Artigiani S, Gilestro G, Barberis D, Tamagnone L,
857 Comoglio PM. 2002. The semaphorin 4D receptor controls invasive growth by
858 coupling with Met. *Nat Cell Biol* **4**: 720-724.
859 Goetz SC, Anderson KV. 2010. The primary cilium: a signalling centre during vertebrate
860 development. *Nat Rev Genet* **11**: 331-344.
861 Gu C, Yoshida Y, Livet J, Reimert DV, Mann F, Merte J, Henderson CE, Jessell TM,
862 Kolodkin AL, Ginty DD. 2005. Semaphorin 3E and plexin-D1 control vascular
863 pattern independently of neuropilins. *Science* **307**: 265-268.
864 Hamburger V, Hamilton HL. 1951. A series of normal stages in the development of the
865 chick embryo. *J Morphol* **88**: 49-92.
866 Haycraft CJ, Banizs B, Aydin-Son Y, Zhang Q, Michaud EJ, Yoder BK. 2005. Gli2 and
867 Gli3 localize to cilia and require the intraflagellar transport protein polaris for
868 processing and function. *PLoS Genet* **1**: e53.
869 He Z, Tessier-Lavigne M. 1997. Neuropilin is a receptor for the axonal chemorepellent
870 Semaphorin III. *Cell* **90**: 739-751.
871 Hillman RT, Feng BY, Ni J, Woo WM, Milenkovic L, Hayden Gephart MG, Teruel MN,
872 Oro AE, Chen JK, Scott MP. 2011. Neuropilins are positive regulators of
873 Hedgehog signal transduction. *Genes Dev* **25**: 2333-2346.
874 Hollway GE, Maule J, Gautier P, Evans TM, Keenan DG, Lohs C, Fischer D, Wicking C,
875 Currie PD. 2006. Scube2 mediates Hedgehog signalling in the zebrafish embryo.
876 *Dev Biol* **294**: 104-118.
877 Holtz AM, Griffiths SC, Davis SJ, Bishop B, Siebold C, Allen BL. 2015. Secreted
878 HHIP1 interacts with heparan sulfate and regulates Hedgehog ligand localization
879 and function. *J Cell Biol* **209**: 739-757.
880 Holtz AM, Peterson KA, Nishi Y, Morin S, Song JY, Charron F, McMahon AP, Allen
881 BL. 2013. Essential role for ligand-dependent feedback antagonism of vertebrate
882 hedgehog signaling by PTCH1, PTCH2 and HHIP1 during neural patterning.
883 *Development* **140**: 3423-3434.
884 Hota PK, Buck M. 2012. Plexin structures are coming: opportunities for multilevel
885 investigations of semaphorin guidance receptors, their cell signaling mechanisms,
886 and functions. *Cell Mol Life Sci* **69**: 3765-3805.
887 Hui CC, Angers S. 2011. Gli proteins in development and disease. *Annu Rev Cell Dev*
888 *Biol* **27**: 513-537.
889 Izzi L, Levesque M, Morin S, Laniel D, Wilkes BC, Mille F, Krauss RS, McMahon AP,
890 Allen BL, Charron F. 2011. Boc and Gas1 each form distinct Shh receptor
891 complexes with Ptch1 and are required for Shh-mediated cell proliferation. *Dev*
892 *Cell* **20**: 788-801.
893 Janssen BJ, Robinson RA, Perez-Branguli F, Bell CH, Mitchell KJ, Siebold C, Jones EY.
894 2010. Structural basis of semaphorin-plexin signalling. *Nature* **467**: 1118-1122.
895 Jeong J, McMahon AP. 2005. Growth and pattern of the mammalian neural tube are
896 governed by partially overlapping feedback activities of the hedgehog antagonists
897 patched 1 and Hhip1. *Development* **132**: 143-154.
898 Jongbloets BC, Pasterkamp RJ. 2014. Semaphorin signalling during development.
899 *Development* **141**: 3292-3297.
900 Kawakami A, Nojima Y, Toyoda A, Takahoko M, Satoh M, Tanaka H, Wada H, Masai I,
901 Terasaki H, Sakaki Y et al. 2005. The zebrafish-secreted matrix protein

you/scube2 is implicated in long-range regulation of hedgehog signaling. *Curr Biol* **15**: 480-488.

Kawakami T, Kawcak T, Li YJ, Zhang W, Hu Y, Chuang PT. 2002. Mouse dispatched mutants fail to distribute hedgehog proteins and are defective in hedgehog signaling. *Development* **129**: 5753-5765.

Kawasaki T, Kitsukawa T, Bekku Y, Matsuda Y, Sanbo M, Yagi T, Fujisawa H. 1999. A requirement for neuropilin-1 in embryonic vessel formation. *Development* **126**: 4895-4902.

Kee HL, Dishinger JF, Blasius TL, Liu CJ, Margolis B, Verhey KJ. 2012. A size-exclusion permeability barrier and nucleoporins characterize a ciliary pore complex that regulates transport into cilia. *Nat Cell Biol* **14**: 431-437.

Kolodkin AL, Levengood DV, Rowe EG, Tai YT, Giger RJ, Ginty DD. 1997. Neuropilin is a semaphorin III receptor. *Cell* **90**: 753-762.

Koropouli E, Kolodkin AL. 2014. Semaphorins and the dynamic regulation of synapse assembly, refinement, and function. *Curr Opin Neurobiol* **27**: 1-7.

Lee CS, Buttitta L, Fan CM. 2001. Evidence that the WNT-inducible growth arrest-specific gene 1 encodes an antagonist of sonic hedgehog signaling in the somite. *Proc Natl Acad Sci U S A* **98**: 11347-11352.

Ma Y, Erkner A, Gong R, Yao S, Taipale J, Basler K, Beachy PA. 2002. Hedgehog-mediated patterning of the mammalian embryo requires transporter-like function of dispatched. *Cell* **111**: 63-75.

Machold R, Hayashi S, Rutlin M, Muzumdar MD, Nery S, Corbin JG, Gritli-Linde A, Dellovade T, Porter JA, Rubin LL et al. 2003. Sonic hedgehog is required for progenitor cell maintenance in telencephalic stem cell niches. *Neuron* **39**: 937-950.

Marigo V, Tabin CJ. 1996. Regulation of patched by sonic hedgehog in the developing neural tube. *Proc Natl Acad Sci U S A* **93**: 9346-9351.

Mauti O, Sadhu R, Gemayel J, Gesemann M, Stoeckli ET. 2006. Expression patterns of plexins and neuropilins are consistent with cooperative and separate functions during neural development. *BMC Dev Biol* **6**: 32.

Megason SG, McMahon AP. 2002. A mitogen gradient of dorsal midline Wnts organizes growth in the CNS. *Development* **129**: 2087-2098.

Muhl L, Folestad EB, Gladh H, Wang Y, Moessinger C, Jakobsson L, Eriksson U. 2017. Neuropilin 1 binds PDGF-D and is a co-receptor in PDGF-D-PDGFRbeta signaling. *J Cell Sci* **130**: 1365-1378.

Mukhopadhyay S, Wen X, Ratti N, Loktev A, Rangell L, Scales SJ, Jackson PK. 2013. The ciliary G-protein-coupled receptor Gpr161 negatively regulates the Sonic hedgehog pathway via cAMP signaling. *Cell* **152**: 210-223.

Neufeld G, Kessler O. 2008. The semaphorins: versatile regulators of tumour progression and tumour angiogenesis. *Nat Rev Cancer* **8**: 632-645.

Neufeld G, Mumblat Y, Smolkin T, Toledano S, Nir-Zvi I, Ziv K, Kessler O. 2016. The semaphorins and their receptors as modulators of tumor progression. *Drug Resist Updat* **29**: 1-12.

Nogi T, Yasui N, Mihara E, Matsunaga Y, Noda M, Yamashita N, Toyofuku T, Uchiyama S, Goshima Y, Kumanogoh A et al. 2010. Structural basis for semaphorin signalling through the plexin receptor. *Nature* **467**: 1123-1127.

Nybakken K, Vokes SA, Lin TY, McMahon AP, Perrimon N. 2005. A genome-wide RNA interference screen in Drosophila melanogaster cells for new components of the Hh signaling pathway. *Nat Genet* **37**: 1323-1332.

Ocbina PJ, Eggenschwiler JT, Moskowitz I, Anderson KV. 2011. Complex interactions between genes controlling trafficking in primary cilia. *Nat Genet* **43**: 547-553.

Perala N, Sariola H, Immonen T. 2012. More than nervous: the emerging roles of plexins. *Differentiation* **83**: 77-91.

Perala NM, Immonen T, Sariola H. 2005. The expression of plexins during mouse embryogenesis. *Gene Expr Patterns* **5**: 355-362.

Petrova R, Joyner AL. 2014. Roles for Hedgehog signaling in adult organ homeostasis and repair. *Development* **141**: 3445-3457.

Pinskey JM, Franks NE, McMellen AN, Giger RJ, Allen BL. 2017. Neuropilin-1 promotes Hedgehog signaling through a novel cytoplasmic motif. *J Biol Chem* **292**: 15192-15204.

Prud'homme GJ, Glinka Y. 2012. Neuropilins are multifunctional coreceptors involved in tumor initiation, growth, metastasis and immunity. *Oncotarget* **3**: 921-939.

Puschel AW. 2007. GTPases in semaphorin signaling. *Adv Exp Med Biol* **600**: 12-23.

Rich SK, Baskar R, Terman JR. 2021. Propagation of F-actin disassembly via Myosin15-Mical interactions. *Sci Adv* **7**.

Rohatgi R, Milenkovic L, Scott MP. 2007. Patched1 regulates hedgehog signaling at the primary cilium. *Science* **317**: 372-376.

Rohm B, Ottemeyer A, Lohrum M, Puschel AW. 2000a. Plexin/neuropilin complexes mediate repulsion by the axonal guidance signal semaphorin 3A. *Mech Dev* **93**: 95-104.

Rohm B, Rahim B, Kleiber B, Hovatta I, Puschel AW. 2000b. The semaphorin 3A receptor may directly regulate the activity of small GTPases. *FEBS Lett* **486**: 68-72.

Roth L, Nasarre C, Dirrig-Grosch S, Aunis D, Cremel G, Hubert P, Bagnard D. 2008. Transmembrane domain interactions control biological functions of neuropilin-1. *Mol Biol Cell* **19**: 646-654.

Sarabipour S, Mac Gabhann F. 2021. Targeting neuropilins as a viable SARS-CoV-2 treatment. *FEBS J*.

Stone DM, Hynes M, Armanini M, Swanson TA, Gu Q, Johnson RL, Scott MP, Pennica D, Goddard A, Phillips H et al. 1996. The tumour-suppressor gene patched encodes a candidate receptor for Sonic hedgehog. *Nature* **384**: 129-134.

Suto F, Tsuboi M, Kamiya H, Mizuno H, Kiyama Y, Komai S, Shimizu M, Sanbo M, Yagi T, Hiromi Y et al. 2007. Interactions between plexin-A2, plexin-A4, and semaphorin 6A control lamina-restricted projection of hippocampal mossy fibers. *Neuron* **53**: 535-547.

Takahashi T, Fournier A, Nakamura F, Wang LH, Murakami Y, Kalb RG, Fujisawa H, Strittmatter SM. 1999. Plexin-neuropilin-1 complexes form functional semaphorin-3A receptors. *Cell* **99**: 59-69.

Takahashi T, Strittmatter SM. 2001. Plexina1 autoinhibition by the plexin sema domain. *Neuron* **29**: 429-439.

Tamagnone L, Artigiani S, Chen H, He Z, Ming GI, Song H, Chedotal A, Winberg ML, Goodman CS, Poo M et al. 1999. Plexins are a large family of receptors for

transmembrane, secreted, and GPI-anchored semaphorins in vertebrates. *Cell* **99**: 71-80.

Teglund S, Toftgard R. 2010. Hedgehog beyond medulloblastoma and basal cell carcinoma. *Biochim Biophys Acta* **1805**: 181-208.

Tenzen T, Allen BL, Cole F, Kang JS, Krauss RS, McMahon AP. 2006. The cell surface membrane proteins Cdo and Boc are components and targets of the Hedgehog signaling pathway and feedback network in mice. *Dev Cell* **10**: 647-656.

Todaro GJ, Green H. 1963. Quantitative studies of the growth of mouse embryo cells in culture and their development into established lines. *J Cell Biol* **17**: 299-313.

Toyofuku T, Zhang H, Kumanogoh A, Takegahara N, Suto F, Kamei J, Aoki K, Yabuki M, Hori M, Fujisawa H et al. 2004. Dual roles of Sema6D in cardiac morphogenesis through region-specific association of its receptor, Plexin-A1, with off-track and vascular endothelial growth factor receptor type 2. *Genes Dev* **18**: 435-447.

Tukachinsky H, Kuzmickas RP, Jao CY, Liu J, Salic A. 2012. Dispatched and scube mediate the efficient secretion of the cholesterol-modified hedgehog ligand. *Cell Rep* **2**: 308-320.

van den Heuvel M, Ingham PW. 1996. smoothened encodes a receptor-like serpentine protein required for hedgehog signalling. *Nature* **382**: 547-551.

Vyas N, Goswami D, Manonmani A, Sharma P, Ranganath HA, VijayRaghavan K, Shashidhara LS, Sowdhamini R, Mayor S. 2008. Nanoscale organization of hedgehog is essential for long-range signaling. *Cell* **133**: 1214-1227.

Wang Y, He H, Srivastava N, Vikarunnessa S, Chen YB, Jiang J, Cowan CW, Zhang X. 2012. Plexins are GTPase-activating proteins for Rap and are activated by induced dimerization. *Sci Signal* **5**: ra6.

Wang Y, Pascoe HG, Brautigam CA, He H, Zhang X. 2013. Structural basis for activation and non-canonical catalysis of the Rap GTPase activating protein domain of plexin. *Elife* **2**: e01279.

Whalen DM, Malinauskas T, Gilbert RJ, Siebold C. 2013. Structural insights into proteoglycan-shaped Hedgehog signaling. *Proc Natl Acad Sci U S A* **110**: 16420-16425.

Winberg ML, Tamagnone L, Bai J, Comoglio PM, Montell D, Goodman CS. 2001. The transmembrane protein Off-track associates with Plexins and functions downstream of Semaphorin signaling during axon guidance. *Neuron* **32**: 53-62.

Wong SY, Seol AD, So PL, Ermilov AN, Bichakjian CK, Epstein EH, Jr., Dlugosz AA, Reiter JF. 2009. Primary cilia can both mediate and suppress Hedgehog pathway-dependent tumorigenesis. *Nat Med* **15**: 1055-1061.

Woods IG, Talbot WS. 2005. The you gene encodes an EGF-CUB protein essential for Hedgehog signaling in zebrafish. *PLoS Biol* **3**: e66.

Yan D, Lin X. 2008. Opposing roles for glypicans in Hedgehog signalling. *Nat Cell Biol* **10**: 761-763.

Yang T, Terman JR. 2013. Regulating small G protein signaling to coordinate axon adhesion and repulsion. *Small GTPases* **4**: 34-41.

Yazdani U, Terman JR. 2006. The semaphorins. *Genome Biol* **7**: 211.

1038 Yoshida Y, Han B, Mendelsohn M, Jessell TM. 2006. PlexinA1 signaling directs the
1039 segregation of proprioceptive sensory axons in the developing spinal cord.
1040 *Neuron* **52**: 775-788.
1041 Zhang XM, Ramalho-Santos M, McMahon AP. 2001. Smoothened mutants reveal
1042 redundant roles for Shh and Ihh signaling including regulation of L/R asymmetry
1043 by the mouse node. *Cell* **105**: 781-792.
1044 Zhao XF, Kohen R, Parent R, Duan Y, Fisher GL, Korn MJ, Ji L, Wan G, Jin J, Puschel
1045 AW et al. 2018. PlexinA2 Forward Signaling through Rap1 GTPases Regulates
1046 Dentate Gyrus Development and Schizophrenia-like Behaviors. *Cell Rep* **22**: 456-
1047 470.

1048